

Integrated Ocean Drilling Program Expedition 335 Scientific Prospectus

Superfast Spreading Rate Crust 4

Damon A.H. Teagle

Co-Chief Scientist
School of Ocean and Earth Science
University of Southampton
National Oceanography Centre, Southampton
European Way
Southampton, SO14-3ZH
United Kingdom

Benoit Ildefonse

Co-Chief Scientist
Géosciences Montpellier
CNRS—Université Montpellier 2
CC 60, Place Eugène Bataillon
34095 Montpellier Cedex 05
France

Peter Blum

Expedition Project Manager/Staff Scientist
Integrated Ocean Drilling Program
Texas A&M University
College Station TX 77845
USA



Published by
Integrated Ocean Drilling Program Management International, Inc.,
for the Integrated Ocean Drilling Program

Publisher's notes

Material in this publication may be copied without restraint for library, abstract service, educational, or personal research purposes; however, this source should be appropriately acknowledged.

Citation:

Teagle, D.A.H, Ildefonse, B., and Blum, P., 2010. Superfast spreading rate crust 4. *IODP Sci. Prosp.*, 335. doi:10.2204/iodp.sp.335.2010

Distribution:

Electronic copies of this series may be obtained from the Integrated Ocean Drilling Program (IODP) Scientific Publications homepage on the World Wide Web at www.iodp.org/scientific-publications/.

This publication was prepared by the Integrated Ocean Drilling Program U.S. Implementing Organization (IODP-USIO): Consortium for Ocean Leadership, Lamont-Doherty Earth Observatory of Columbia University, and Texas A&M University, as an account of work performed under the international Integrated Ocean Drilling Program, which is managed by IODP Management International (IODP-MI), Inc. Funding for the program is provided by the following agencies:

National Science Foundation (NSF), United States

Ministry of Education, Culture, Sports, Science and Technology (MEXT), Japan

European Consortium for Ocean Research Drilling (ECORD)

Ministry of Science and Technology (MOST), People's Republic of China

Korea Institute of Geoscience and Mineral Resources (KIGAM)

Australian Research Council (ARC) and New Zealand Institute for Geological and Nuclear Sciences (GNS), Australian/New Zealand Consortium

Ministry of Earth Sciences (MoES), India

Disclaimer

Any opinions, findings, and conclusions or recommendations expressed in this publication are those of the author(s) and do not necessarily reflect the views of the participating agencies, IODP Management International, Inc., Consortium for Ocean Leadership, Lamont-Doherty Earth Observatory of Columbia University, Texas A&M University, or Texas A&M Research Foundation.

This IODP *Scientific Prospectus* is based on precruise Science Advisory Structure panel discussions and scientific input from the designated Co-Chief Scientists on behalf of the drilling proponents. During the course of the cruise, actual site operations may indicate to the Co-Chief Scientists, the Staff Scientist/Expedition Project Manager, and the Operations Superintendent that it would be scientifically or operationally advantageous to amend the plan detailed in this prospectus. It should be understood that any proposed changes to the science deliverables outlined in the plan presented here are contingent upon the approval of the IODP-USIO Science Services, TAMU, Director in consultation with IODP-MI.

Abstract

Integrated Ocean Drilling Program (IODP) Expedition 335 (14 April–4 June 2011) will be the fourth ocean cruise of the “Superfast” campaign to drill a deep hole into intact oceanic basement and will return to Ocean Drilling Program (ODP) Hole 1256D to deepen this scientific reference penetration a significant distance into cumulate gabbros. Cores and data recovered during the Superfast 4 expedition will provide hitherto unavailable observations that will test models of the accretion and evolution of the oceanic crust. Site 1256 was specifically located on oceanic crust that formed at a superfast spreading rate (>200 mm/y) to exploit the observed relationship between spreading rate and depth to axial low velocity zones, thought to be magma chambers, seismically imaged at active mid-ocean ridges. This was a deliberate strategy to reduce the drilling distance to gabbroic rocks because thick sequences of lavas and dikes have proved difficult to penetrate in past. ODP Leg 206 (2002) initiated operations at Site 1256, including the installation in Hole 1256D of a reentry cone with 16 inch casing inserted through the 250 m thick sedimentary cover and cemented into basement to facilitate deep drilling. The hole was then cored ~500 m into basement. IODP Expeditions 309 and 312 (2005) successfully completed the first sampling of an intact section of upper oceanic crust from lavas, through the sheeted dikes, and into the upper gabbros. Hole 1256D now penetrates >1500 meters below seafloor (mbsf) and >1250 m subbasement and currently resides in the dike–gabbro transition zone. The first gabbroic rocks were encountered at 1407 mbsf. Below this lies a ~100 m complex zone of fractionated gabbros intruded into contact metamorphosed dikes.

Although previous cruises achieved the benchmark objective of reaching gabbro in intact ocean crust, critical scientific questions remain. These include the following:

1. Does the lower crust form by the recrystallization and subsidence of a high-level magma chamber (gabbro glacier), crustal accretion by intrusion of sills throughout the lower crust, or some other mechanism?
2. Is the plutonic crust cooled by conduction or hydrothermal circulation?
3. What is the geological nature of Layer 3 and the Layer 2/3 boundary at Site 1256?
4. What is the magnetic contribution of the lower crust to marine magnetic anomalies?

Hole 1256D is poised at a depth where samples that should conclusively address these questions can be obtained, possibly with only a few hundred meters of drilling. Importantly, as of the end of Expedition 312, the hole was clear of debris and open to its

full depth. Increased rates of penetration (1.2 m/h) and enhanced core recovery (>35%) in the gabbros indicate that this return to Hole 1256D could deepen the hole >300 m into plutonic rocks, past the transition from dikes to gabbro, and into a region of solely cumulate gabbroic rocks.

Schedule for Expedition 335

Expedition 335 is based on Integrated Ocean Drilling Program (IODP) drilling proposal number 522Full5 (available at iodp.tamu.edu/scienceops/expeditions/superfast_rate_crust.html). Following ranking by the IODP Scientific Advisory Structure, the expedition was scheduled for the research vessel *JOIDES Resolution*, operating under contract with the U.S. Implementing Organization. At the time of publication of this *Scientific Prospectus*, the expedition is scheduled to start in Balboa, Panama, on 14 April 2011 and to end in Colón, Panama, on 4 June 2011. A total of 39 days will be available for the drilling, coring, and downhole measurements described in this prospectus (for the current detailed schedule, see iodp.tamu.edu/scienceops/). Further details about the facilities aboard the *JOIDES Resolution* and the USIO can be found at www.iodp-usio.org/.

Introduction

Drilling a complete in situ section of ocean crust has been an unfulfilled ambition of Earth scientists since the inception of ocean drilling. Unfortunately, many of the key questions and primary scientific goals of the IODP Initial Science Plan regarding the formation and evolution of the oceanic crust remain unanswered despite more than 40 years of scientific ocean drilling. This is principally due to cursory sampling of the ocean crust (see Teagle et al., 2004; Wilson, Teagle, Acton, et al., 2003). Fundamental advances in our knowledge of mid-ocean-ridge accretion will be achieved by deepening Hole 1256D a significant distance (i.e., several hundreds of meters) into cumulate gabbro.

Although offset drilling strategies, where deeper parts of the ocean crust are sampled by drilling in tectonic windows, have had notable success at Hess Deep (Gillis, Mével, Allan, et al., 1993), on the Southwest Indian Ridge (Dick, Natland, Miller, et al., 1999), or on the Mid-Atlantic Ridge (Cannat, Karson, Miller, et al., 1995; Kelemen, Kikawa, Miller, et al., 2004; Blackman, Ildfonse, John, Ohara, Miller, MacLeod, et al., 2006), composite sections of ocean crust are not substitutes for long continuous drill holes

into intact crust far from fracture zones. Only by drilling intact sections of ocean crust will we be able to estimate the bulk composition of the crust, establish the chemical connections between lavas and melts coming from the mantle, test competing models of lower crustal magmatic accretion, understand the extent and intensity of hydrothermal exchange between the ocean crust and the seawater, calibrate regional seismic measurements, understand the origin of magnetic anomalies, and make estimates of the chemical fluxes returned to the mantle by the subduction of the oceanic lithosphere. Basic observations regarding the architecture of ocean crust, including the rock types; the geochemistry and thicknesses of the volcanic, dike, and plutonic sections; and the nature of the Moho itself, are yet to be made. Sampling through drilling, coupled with detailed geophysical experiments, remain essential to correlate geochemical, seismic, and magnetic imaging of the ocean crust with basic geologic observations.

Although only 20% of modern ridges are moving apart at fast spreading rates (>80 mm/y full rate), ~50% of present-day ocean crust and ~30% of the Earth's surface was produced by this pace of spreading. The great majority of crust subducted back into the mantle during the last 200 m.y. formed at fast spreading ridges. Fast spread ocean crust is believed to be less variable than crust formed at slower spreading rates and closer to the ideal "Penrose" pseudostratigraphy developed from ophiolites (Anonymous, 1972). Hence, understanding accretion processes at a few sites might reasonably be extrapolated to describe a significant portion of the Earth's surface. Importantly, we already have well-developed theoretical models of competing styles of magmatic accretion in fast spreading ridges (e.g., gabbro glaciers versus sheeted sills), and methods have been developed to test these models. However, these hypotheses will be best tested using samples recovered from drilling intact sections of ocean basement.

The "Superfast" campaign has already achieved one of the major unfulfilled goals of ocean drilling—namely, the sampling of a complete section from lavas, through the dikes, and into gabbros. This was accomplished by drilling Hole 1256D in crust that formed at a superfast spreading rate at the East Pacific Rise (EPR) ~15 m.y. ago (Fig. F1). Drilling took place during three scientific ocean drilling cruises: Ocean Drilling Program (ODP) Leg 206 (Wilson, Teagle, Acton, et al., 2003) and IODP Expeditions 309 and 312 (Expedition 309 Scientists, 2005; Expedition 309/312 Scientists, 2006; Teagle, Alt, Umino, Miyashita, Banerjee, Wilson, et al., 2006; Wilson et al., 2006). The base of the hole resides within the dike-gabbro transition zone. In situ cumulate gabbros from intact ocean crust are now within reach of scientific ocean drilling.

Background

Developing a comprehensive understanding of the accretion of new crust at mid-ocean ridges requires samples of cumulate gabbro, as it is these coarsely crystalline rocks that hold records of the deep magmatic, hydrothermal, and tectonic processes that dominate in the lower crust. Gabbros make up >65% of the oceanic crust but lie beneath 1000 to 2000 m of lavas and dikes in typical “Penrose”-type ocean crust. Past drilling of the upper oceanic crust (e.g., Deep Sea Drilling Project [DSDP] Hole 504B; Alt, Kinoshita, Stokking, et al., 1993) has been fraught with problems of low core recovery, poor hole conditions, and equipment failure, all because of the hard and highly fractured nature of magmas erupted onto or intruded at shallow levels into the oceanic crust. The Superfast campaign developed from the idea of minimizing the thickness of upper crustal rocks to be cored before sampling gabbros.

There is an observed relationship between spreading rate and the depth of axial low-velocity zones, thought to be magma chambers, imaged by multichannel seismic (MCS) experiments at active ridge crests (Fig. F2) (Purdy et al., 1992). Reconsideration of magnetic anomalies formed at the southern end of the Pacific/Cocos plate boundary identified crust formed at a full spreading rate of ~220 mm/y from 20 to 11 Ma (Wilson, 1996) (Fig. F1). This is significantly faster than the present fastest spreading rate (~145 mm/y) for crust forming at ~20°–30°S on the EPR. From this region created by superfast spreading, a single drill site in the Guatemala Basin, initially designated GUATB-03C (Fig. F3) and now known as Site 1256, was selected on ~15 m.y. old ocean crust. At this site, gabbroic rocks were predicted to occur between 1275 and 1550 meters below seafloor (mbsf), assuming a typical carapace of 300 m of off-axis lavas (Expedition 309 Scientists, 2005; Teagle, Alt, Umino, Miyashita, Banerjee, Wilson, et al., 2006). This approach and site was endorsed by the ODP “Architecture of the Oceanic Lithosphere Program Planning Group” (1998; available online at www.iodp.org/mission-moho-workshop/) as the optimum location to pursue major science goals in fast spreading rate crust.

ODP Hole 1256D in the eastern equatorial Pacific is the first basement borehole prepared with the infrastructure desirable for drilling a moderately deep hole into oceanic crust (~1.5–2 km). ODP Leg 206 installed a reentry cone supported by 20 inch casing with large-diameter (16 inch) casing through 250 m of sediment and cemented 19 m into basement. The cone and casing allow multiple reentries and maintain hole stability, essential for deep drilling. The wide-diameter casing allows for two further casing strings (13³/₈ and 10³/₄ inches) to be installed in the well, should future bore-

hole stabilization be required and appropriate technology be available. Following the initiation of Hole 1256D, 502 m of massive lavas and sheet flows with moderate to high recovery were penetrated during Leg 206 (48%; Wilson, Teagle, Acton, et al., 2003). During Expeditions 309 and 312 (July–August and November–December 2005, respectively), Hole 1256D was successfully deepened to a total depth of 1507.1 mbsf, with the lower ~100 m hosted by a zone of gabbroic sills intruded into contact metamorphosed dikes (Fig. F4) (Wilson et al., 2006; Teagle, Alt, Umino, Miyashita, Banerjee, Wilson, et al., 2006).

In addition to the shallow depth to gabbros predicted from formation at a superfast spreading rate, Site 1256 has a number of specific attributes that indicate this site provides an excellent opportunity to sample a complete section of upper oceanic crust. The crust at Site 1256 formed near the Equator (Fig. F5), and high equatorial productivity resulted in high sedimentation rates (>30 m/m.y.) (Farrell et al., 1995) and the rapid burial of the young basement. A thick sediment blanket was needed for the installation of a reentry cone with 20 inch casing that forms the foundation for deployment of the second 16 inch diameter casing string that was cemented 19 m into the uppermost basement. At 15 Ma, Site 1256 is significantly older than the crust in Hole 504B (6.9 Ma; Alt, Kinoshita, Stokking, et al., 1993), and lower temperatures are anticipated at mid-levels of the crust. Logistically, Site 1256 has a number of advantages. It has a 12-month weather window and is ~3.5 days steaming from the Panama Canal; the short transit time allows for maximum time on site during drilling expeditions.

Site surveys and the geological setting of Hole 1256D

Site 1256 (6°44.2'N, 91°56.1'W) lies in 3635 m of water in the Guatemala Basin on Cocos plate crust formed ~15 m.y. ago on the eastern flank of the EPR (Figs. F1, F5). The details of site survey operations and the reasons for the selection of this particular site are outlined in detail in Wilson, Teagle, Acton, et al. (2003). Supporting site survey data for Expedition 335 and previous drilling at Site 1256 are archived at the [IODP Site Survey Data Bank](#). Three regions were surveyed during the 1999 *Maurice Ewing* site survey cruise (Hallenborg et al., 2003; Wilson et al., 2003), with Site C in the GUATB-03 region selected as the preferred location for deep drilling (Fig. F3) (Wilson, Teagle, Acton, et al., 2003). The depth of the site is close to that predicted from bathymetry models of plate cooling (e.g., Parsons and Sclater, 1977). The site sits astride the magnetic anomaly 5Bn–5Br transition in magnetic polarity (Fig. F3). This crust accreted at a superfast spreading rate (~220 mm/y full rate) (Wilson, 1996) and lies ~1150 km east of the present crest of the EPR and ~530 km north of the Cocos

Ridge. The site formed on a ridge segment at least 400 km in length, ~100 km north of the ridge-ridge-ridge triple junction between the Cocos, Pacific, and Nazca plates (Fig. F5). This location was formed near the Equator within the equatorial high-productivity zone and initially endured high sedimentation rates (>30 m/m.y.) (e.g., Farrell et al., 1995; Wilson, Teagle, Acton, et al., 2003). Sediment thickness in the region is between 200 and 300 m and is 250 m at Site 1256 (Wilson, Teagle, Acton, et al., 2003).

Site 1256 has a seismic structure reminiscent of typical Pacific off-axis seafloor (Fig. F6). Upper Layer 2 velocities are 4.5–5 km/s and the Layer 2–3 transition is between ~1200 and 1500 m subbasement (Fig. F7). The total crustal thickness at Site 1256 is estimated at ~5–5.5 km. Further to the northeast of Site 1256 (15–20 km), a trail of ~500 m high circular seamounts rise a few hundred meters above the sediment blanket (Fig. F3B). Bathymetry in the GUATB-03 survey areas is generally subdued, and Site 1256 sits atop a region of smooth basement topography (<10 m relief). However, elsewhere in the region, the top of basement shows a number of offsets along north-west-striking normal faults, and an abyssal hill relief of as much as 100 m is apparent in the southwest part of the area. Relief to the northeast is lower and less organized. In the northeastern sector of the GUAT-3B region, there is evidence for a basement thrust fault with a strike approximately orthogonal to the regional fabric (Wilson et al., 2003; Hallenborg et al., 2003). This feature dips gently to the northwest ($\sim 15^\circ$) and is clearly discernible to a depth of ~1.3 km on seismic Line EW9903-28 (Wilson et al., 2003), but the feature is less pronounced on seismic Line EW9903-27, indicating that the offset on the thrust decreases to the southwest.

Additional processing (A.J. Harding, unpubl. data) of ocean bottom hydrophone (OBH) recordings indicates discernible variation in the average seismic velocity (~ 4.54 – 4.88 km/s) of the uppermost (~100 m) basement and that there is regional coherence in the velocity variations (Fig. F8A). Two principal features are apparent: a 5 to 10 km wide zone of relatively high upper basement velocities (>4.82 km/s) that can be traced ~20 km to the edge of data coverage southeast of Site 1256 and a relatively low velocity (4.66–4.54 km/s) bull's-eye centered around the crossing point of seismic Lines EW9903-21 and 25. Using the site survey MCS data (Wilson et al., 2003), we have constructed a geological sketch map of the uppermost basement in the GUATB-03 survey region (Fig. F8B). The uppermost basement at Site 1256 is capped by a massive lava flow >74 m thick (Fig. F4). This flow is relatively unfractured, with shipboard physical properties measurements on discrete samples indicating $V_P > 5.5$ km/s (Wilson, Teagle, Acton, et al., 2003). As such, it is likely that the area of relatively high up-

permost basement seismic velocities represents the extent of the massive flow penetrated during Leg 206 in Holes 1256C and 1256D. Assuming an average thickness of 40 m, this would conservatively suggest an eruption volume in excess of 3 km³, plausibly >10 km³. This volume is extremely large when compared to the size of mid-ocean-ridge axial low-velocity zones, which are thought to be high-level melt lenses with typical volumes ~0.05–0.15 km³ per kilometer of ridge axis and generally appearing to be only partially molten (Singh et al., 1998).

Sheet flows (<3 m thick) and massive flows (>3 m) make up most of the lava stratigraphy cored so far at Site 1256, and such lava morphologies have been shown to dominate crust formed at fast spreading rates, away from segment tips (e.g., White et al., 2000, 2002). Subordinate pillow lavas are present in Hole 1256D, and because of the large number of fractures and pillow interstices, seismic velocities in these units are generally lower than those in more massive lava flows. We speculate that the bull's-eye of relatively low seismic velocities is a thick pile of dominantly pillowed lava flows.

Highlights of deep drilling in Hole 1256D

The uppermost crust at Site 1256 comprises a ~100 m thick sequence of lava dominated by a single massive lava flow up to 75 m thick, requiring at least this much seafloor relief to pond the lava. On modern fast spreading ridges, such topography does not normally develop until 5–10 km from the axis (Macdonald et al., 1996). Although this lava flow cooled off-axis, it may have originated at the ridge axis before flowing onto the ridge flanks, as is observed for very large lava flows on the modern ocean floor (Macdonald et al., 1989). The lavas immediately below include sheet and massive flows, along with minor pillow flows. Subvertical, elongate flow-top fractures filled with quenched glass and hyaloclastite in these lavas indicate flow lobe inflation, requiring cooling on a subhorizontal surface off-axis (Umino et al., 2000). From this shipboard evidence, we estimated a total thickness of 284 m of lavas that flowed and cooled off-axis. Sheet flows and massive lavas erupted at the ridge axis make up the remaining extrusive section down to 1004 mbsf before a lithologic transition is marked by subvertical intrusive contacts and mineralized breccias. This stratigraphy contrasts slightly with the volcanic stratigraphy for Hole 1256D developed from analysis of wireline geophysical imaging (Tominaga et al., 2009; Tominaga and Umino, 2010), which suggests <50% of the lavas drilled crystallized within 1000 m of the axis but that the majority of the lava pile had formed within 3000 m of the ridge crest.

Below 1061 mbsf, subvertical intrusive contacts are numerous, indicating the start of a relatively thin ~350 m thick sheeted dike complex dominated by massive basalts. Some basalts have doleritic textures, and many are cross-cut by subvertical dikes with common strongly brecciated and mineralized chilled margins. There is no evidence from core or from geophysical wireline logs for significant tilting of the dikes, consistent with subhorizontal seismic reflectors in the lower extrusive rocks that are continuous for several kilometers across the site (Hallenborg et al., 2003). Measurements of dike orientations by wireline imaging are in close agreement with direct measurements on recovered cores and indicate that the dikes at Site 1256 are slightly tilted away from the paleospreading axis (dip and dip direction are $79^\circ \pm 8^\circ/\text{N}053 \pm 23$, respectively) (Tominaga et al., 2009).

The secondary mineralogy of the rocks indicates a stepwise increase in alteration grade downhole from the lavas to the dikes, with low-temperature phases (<150°C phyllosilicates and iron oxyhydroxides) in the lavas giving way to dikes partially altered to chlorite and other greenschist facies minerals (at temperatures greater than ~250°C) (Fig. F4) (also see Alt et al., 2010). Within the dikes, alteration intensity and grade increase downhole, with actinolite more abundant than chlorite below 1300 mbsf and hornblende present below 1350 mbsf, indicating temperatures approaching ~400°C (Alt et al., 2010). The dikes have significantly lower porosity (mostly 0.5%–2%) and higher *P*-wave velocities and thermal conductivity than the lavas, and porosity decreases and *P*-wave velocity increases with depth in the dikes.

In the lower ~60 m of the sheeted dikes (1348–1407 mbsf), basalts are partially to completely recrystallized to distinctive granoblastic textures characterized by granular secondary clinopyroxene and lesser orthopyroxene resulting from contact metamorphism by underlying gabbroic intrusions (Figs. F4, F9A) (Koepke et al., 2008; Alt et al., 2010). Aside from the granoblastic contact metamorphic assemblages in the basal dikes, hydrothermal mineralogy and inferred alteration temperatures of the lower dikes in Hole 1256D are generally similar to those in the lower dikes of Hole 504B (as high as ~400°C). The much thinner dike section at Site 1256 than at Site 504 (~350 versus ~1000 m), however, indicates a much steeper hydrothermal temperature gradient at Site 1256 (~0.5°C/m versus 0.16°C/m in Hole 504B).

Gabbro and trondjemite dikes intrude into sheeted dikes at 1407 mbsf, marking the top of the plutonic complex (Fig. F9). Two major bodies of gabbro were penetrated beneath this contact, with the 52 m thick upper gabbro (Gabbro 1) separated from the 24 m thick lower gabbro (Gabbro 2) by a 24 m screen of granoblastic dikes (Figs. F4,

F9). The textures and rock types observed in Hole 1256D are reminiscent of varitextured gabbros thought to represent a frozen melt lens beneath the sheeted dike complex and above the cumulate rocks in many ophiolites (e.g., MacLeod and Yaouancq, 2000; France et al., 2009).

Gabbro 1 is mineralogically and texturally heterogeneous, comprising gabbros, oxide gabbros, quartz-rich oxide diorites, and small trondjemite dikelets. Oxide abundance decreases irregularly downhole, and olivine is present in significant amounts only in the lower part of the upper gabbros. These rocks are moderately to highly altered by hydrothermal fluids to actinolitic hornblende, secondary plagioclase, epidote, chlorite, prehnite, and laumontite.

The intervening dike screen is an interval of sheeted dikes captured between the two intrusions of gabbros. The dike screen consists of fine-grained metabasalts similar to the granoblastic dikes overlying the upper gabbros. The dike screen is cut by a number of small quartz gabbro and tonalite dikelets of variable thickness (1–10 cm), grain size, and composition.

Gabbro 2 comprises gabbro, oxide gabbro, and subordinate orthopyroxene-bearing gabbro and trondjemite that are similarly altered to Gabbro 1 and has clear intrusive contacts with the overlying granoblastic dike screen. Partially resorbed stoped dike clasts are entrained within both the upper and lower margins of Gabbro 2 (Fig. **F9G**). Gabbro 2 is characterized by an absence of fresh olivine, high but variable orthopyroxene contents (5%–25%), and considerable local heterogeneity. Oxide abundance generally diminishes downhole. The predominant rock type is orthopyroxene-bearing gabbro with gabbronorite in the marginal units. The lowermost rock recovered from Hole 1256D is a highly altered actinolite-bearing basaltic dike that lacks granoblastic textures and hence is interpreted to be a late dike that postdates the intrusion of the lower gabbro.

Relative to other well-studied upper ocean crust sections (e.g., Karson, 2002), Site 1256 shows a thick lava sequence and a thin dike sequence. Steady-state thermal models require that the conductive lid separating magma from rapidly circulating seawater thin as spreading rate increases, indicating that the thin dike sequence is a direct consequence of the high spreading rate. A thick flow sequence with many massive individual flows and few pillow lavas is a reasonable consequence of short vertical transport distance from the magma chamber and is similar to observations from the midsegments of the fastest spreading ridges in the modern ocean (White et

al., 2002). This model is in direct contrast to spreading models developed from observations of tectonically disrupted fast spread crust exposed in Hess Deep (Karson et al., 2002), which suggest regions of high magma supply should have thin lavas and thick dikes. There is little evidence for tilting (at most a few degrees) in Hole 1256D and no evidence for significant faulting. In contrast, the upper crust exposed at Hess Deep shows significant faulting and rotations within the dike complex (Karson et al., 2002), indicating that observations from that tectonic window might not be widely applicable. The massive lava flow at the top of the Site 1256 basement indicates that faults with ~50–100 m throws must exist relatively near to the ridge axis, even in superfast spreading rate crust, to provide the necessary relief to pond of the lava. At fast spreading ridges such relief is typically developed ~5 to 10 km from the axis.

Marine seismologists have long been dividing the ocean crust into seismic layers: Layer 1 comprises low-velocity sediments, Layer 2 has low-velocity and high-velocity gradient, and Layer 3 has high-velocity (generally at least 6.7 km/s) and low-velocity gradient. There is a widespread perception that Layer 3 is equivalent to gabbro, even though Hole 504B has penetrated Layer 3 but not gabbro (Alt et al., 1996; Detrick et al., 1994). From regional seismic refraction data, the transition from seismic Layer 2 to Layer 3 at Site 1256 occurs at ~1450–1750 mbsf (1200–1500 meters subbasement [msb]) (Wilson et al., 2003) (Fig. F7). Shipboard determinations of seismic velocities of discrete samples are in close agreement with in situ measurements by wireline tools, and gabbro velocities are <6.5 km/s (also Swift et al., 2008). Contrary to expectation, porosity increases and *P*-wave velocities decrease stepwise downward from lowermost dikes into uppermost gabbro in Hole 1256D as the result of the contact metamorphism of the granoblastic dikes and the strong hydrothermal alteration of the uppermost gabbros (Fig. F4). Porosity and velocity then increase downhole in the gabbro but are still <6.5 km/s. Wireline velocity measurements end at the top of gabbro, but we interpret the gabbro intervals as being within Layer 2 because a smoothed extrapolation of the downhole velocities will either have velocities <6.5 km/s, still characteristic of Layer 2, or an exceptionally high gradient to higher velocities, also characteristic of Layer 2. Encountering gabbro at a depth clearly within Layer 2 reinforces previous suggestions that factors including porosity and alteration are more important than rock type or grain size to controlling the location of the Layer 2/3 boundary. The position of the dike/gabbro boundary therefore appears to have little control over the seismic velocity structure of the crust (Alt et al., 1996; Detrick et al., 1994). Unfortunately, because the transition from Layer 2 to Layer 3 lies beneath Hole 1256D, we cannot yet determine what controls this transition at Site 1256.

Geochemistry of magmas from Site 1256

Flows and dikes from Hole 1256D show a wide range of magmatic fractionation, from fairly primitive to evolved (Figs. F4, F10). Shallower than 600 mbsf, magma compositions are bimodal, with relatively evolved thick flows and more primitive thin flows. The lava pond includes rocks with the highest incompatible element compositions (Zr, TiO₂, Y, and V) and lowest compatible element concentration (Cr and Ni), suggesting that it is more evolved than other basalts from Site 1256. The initial division (based on Leg 206 lavas only) into high Zr-TiO₂, low Zr-TiO₂, and high Zr disappears with more data from Expedition 309 and 312. Rare samples from the lava pond fall off the dominant Y versus Zr and TiO₂ versus Zr trends, suggesting possible minor variation in source compositions.

Downhole geochemical compositions of dikes are variable and do not define trends. Primary and evolved compositions are closely juxtaposed as would be expected for vertically intruded magmas. The range of major element compositions in the dikes is similar to the overlying rocks, and the average composition of the dikes is indistinguishable from the average composition of the lavas (e.g., Fig. F5).

The gabbros have highly variable bulk compositions. The uppermost gabbros have geochemical characteristics similar to the overlying dikes with mid-ocean-ridge basalt (MORB) chemistries (MgO ~7–8 wt%; Zr ~47–65 ppm). Conversely, deeper in Gabbro 2 the rocks are significantly less fractionated, and there are general downhole trends of increasing MgO, CaO, and Ni and decreasing FeO, Zr, and Y. The uppermost rocks of Gabbro 2 are fractionated with MgO contents of 6.1 wt%, but lower in the sequence MgO reaches 9.3 wt%. Decreasing concentrations of FeO and TiO₂ downhole suggest that Gabbro 2 is fractionated similarly to Gabbro 1. The intrusive nature of both gabbro bodies and the chemical variations within them suggest that they intruded into the base of the sheeted dikes and underwent minor internal fractionation in situ, resulting in the observed general geochemical stratification.

Although there is scatter in the shipboard data, there are linear trends between MgO versus TiO₂, FeO, CaO, Na₂O, and Zr, most likely resulting from fractional crystallization of a gabbro, with the fractionating assemblage consisting of clinopyroxene and plagioclase, as expected for relatively evolved basaltic magmas. The predicted composition of the cumulate gabbros generated during this fractional crystallization is very different to that of the gabbros drilled so far. Simple mass balance calculations indicate that the average basalt has lost >30% of its original liquid mass as solid gabbro,

implying the presence of at least 300 m of cumulate gabbro in the crust below the present base of the hole.

Gabbro compositions span a range similar to the flows and dikes but are on average more primitive, with higher MgO and lower FeO, albeit still within the range of EPR basalts (Fig. F10). Even though less fractionated, the average gabbro composition is evolved relative to candidates for primary magma in equilibrium with mantle olivine. Possible primary mantle melt compositions should have Mg# of 70–78 and MgO of 9–14 wt%. All flows and dikes and most gabbros are too evolved to be candidates for primary magmas. Therefore, the residue removed from primary magma to produce the observed gabbro and basalt compositions must occur below the present base of Hole 1256D.

The compositional ranges of fresh lava and dike samples correspond to typical values for MORB for most major elements and many trace elements (Su and Langmuir, 2003) and are similar to those observed for the northern EPR (Fig. F10). A few incompatible elements, including Na and Zr, have lower concentrations than those observed for modern EPR lavas, but the generally substantial overlap of compositions indicates that a similar process operated at the superfast spreading ridge that formed Site 1256 and the modern EPR. When trace elements are compared to EPR MORB, they are within one standard deviation of average, albeit on the relatively trace element depleted side of MORB. For example, compared with first-order mid-ocean-ridge segments along the EPR, basalts from Site 1256 have low Zr/TiO₂ and Zr/Y. Although there is overlap among the segments and a large scatter in the data for each segment, Zr/TiO₂ and Zr/Y appear to decrease with increasing spreading rate. The origin of this relationship remains unclear. Spreading rate may affect the extents of magma fractionation or partial melting of the mantle, or it may instead reflect regional-scale mantle heterogeneity. To decrease trace element ratios to this extent would require ~30% more melting at the superfast ridge, but this appears unlikely because of normal crustal thickness (~5.5 km) at Site 1256 (see Park et al., 2008).

The simplest model for mid-ocean-ridge magma plumbing is that the melt lens imaged by MCS experiments is the magma chamber where crystal-rich residues are separated from the evolved lavas that reach the seafloor (Fig. F11). Hole 1256D gabbros are texturally and compositionally similar to varitextured gabbros at the base of the sheeted dike complex in Oman interpreted to represent axial melt lenses (MacLeod and Yaouancq, 2000; France et al., 2009). If the gabbro bodies so far encountered in Hole 1256D were intruded on-axis and if they extended roughly horizontally for at

least hundreds of meters, at 52 and 24 m thick they would have dimensions appropriate for axial low-velocity zones imaged by MCS experiments at intermediate to fast spreading ridges (Singh et al., 1998). However, these bodies could not have been the sites of primary magmatic fractionation. Chilled margins against the underlying dike screens preclude segregating a crystal residue that subsides to form the lower crust as in the gabbro glacier model, and its overall fractionated composition requires that crystals have been segregated elsewhere. This implies that sills or other bodies containing cumulate materials must exist deeper in the crust and/or below the crust/mantle boundary, consistent with recent models based on lower crustal sections of ophiolites (e.g., Boudier et al., 1996; Kelemen et al., 1997; MacLeod and Yaouancq, 2000) and some marine geophysical experiments (Crawford and Webb, 2002; Dunn et al., 2001; Garmany, 1989; Nedimovic et al., 2005; Canales et al., 2009). However, the gabbro glacier mode of accretion, or a combination of the gabbro glacier and sheeted sills models, cannot yet be rejected, as fractionated gabbros in the dike-gabbro transition are not unexpected and the predicted region of cumulate rocks could still exist just below the present maximum depth of Hole 1256D. Deepening Hole 1256D by as little as a few hundred meters would provide the critical samples that enable answering this outstanding basic question.

Scientific objectives

To date, the Superfast campaign has accomplished the significant initial operational objective of drilling a section of intact upper ocean crust down into gabbros. This is a major scientific and engineering achievement, but with only ~100 m penetration into a complicated dike/gabbro boundary transition zone, many scientific objectives of the Superfast mission remain unfulfilled. Before we outline specific objectives for operations in Hole 1256D it is informative to predict what might be encountered with deeper drilling at this site.

What rocks are to be expected with deeper drilling?

With deeper drilling, Hole 1256D will explore unknown territory; hence we must use geological analogs to predict what rocks underlie the current base of Hole 1256D. Field mapping from the lower crust of the Oman ophiolite (e.g., Kelemen and Aharonov, 1998; MacLeod and Yaouancq, 2000; Nicolas et al., 2000, 2009) and submersible studies and shallow drilling of EPR crust at Hess Deep (e.g., Francheteau et al., 1992; Gillis, 1995; Karson et al., 1992, 2002; Natland and Dick, 1996) may be useful

in this respect. However, because of the difficulties of detailed mapping and sampling using submersibles and remotely operated vehicles and the lack of deep drilling of the dike/gabbro boundary in Hess Deep, the well-exposed outcrops in Oman arguably provide the best available guide to the upper plutonic section of fast spreading ocean crust. With detailed geological mapping from the dike/gabbro boundary down toward the harzburgites of the mantle (MacLeod and Yaouancq, 2000) in Wadi Abyad, Oman provides one of the most useful templates of what might be encountered with deeper drilling in Hole 1256D (see also Pallister and Hopson, 1981; Nicolas et al., 1996).

Similar to Hole 1256D, the rocks directly underlying the sheeted dikes complex in Wadi Abyad are varitextured gabbros and microgabbros with subordinate ferrobasalts. The varitextured gabbros are ~150 m thick and show extreme variability in texture, grain size, and chemical composition at centimeter to meter scale and are petrographically very similar to the gabbroic rocks described so far from Hole 1256D. The Oman varitextured gabbros also display a wide range of compositions from those similar to cumulate gabbros to compositions more fractionated than the overlying dikes and lavas (e.g., Mg# 38–82). An average composition weighted according to outcrop abundance indicates that this horizon (Mg# ~65; MacLeod and Yaouancq, 2000) is a pooled basaltic liquid sourced from deeper in the crust (Kelemen and Aharonov, 1998; MacLeod and Yaouancq, 2000; Sinton and Detrick, 1992), similar to the gabbros recovered from Hole 1256D.

The varitextured gabbros grade over a few meters into ~650 m of foliated gabbros with steeply dipping, prominent magmatic foliations oriented subparallel to the strike of the overlying sheeted dikes. These rocks show only weak modal variations. These foliated gabbros pass down into layered gabbros that make up the bulk of the plutonic section in Oman. These layered gabbros exhibit Moho-parallel modal layering defined by variations in the proportion of olivine, clinopyroxene, and plagioclase. Both the foliated and layered gabbros have “cumulate” compositions with high bulk Mg# (>75). Very low P₂O₅ concentrations (<0.02 wt%) indicate low (<5%) proportions of trapped intercumulus liquids. Similar but less detailed observations are recorded from Hess Deep (Francheteau et al., 1992; Gillis, 1995).

Within a few hundred meters of drilling, we anticipate breaching the current dike–gabbro transition zone followed by penetration through a narrow (100–200 m) zone dominated by varitextured gabbros. Below these rocks, we anticipate drilling into cumulate rocks, perhaps with strong subvertical magmatic foliations and only weak

modal layering. Modally layered gabbros with subhorizontal cumulate mineral layers are predicted to occur within 1000 m of the current bottom of Hole 1256D.

Scientific questions

Specific scientific questions that will be addressed by deepening Hole 1256D a significant depth into gabbros include the following:

1. What is the major mechanism of magmatic accretion in crust formed at fast spreading rates? Is the lower crust formed by gabbro glaciers or sheeted sills or by some mixed or unknown mechanism?
2. How is heat extracted from the lower oceanic crust?
3. What is the geological significance of the seismic Layer 2/3 boundary at Site 1256?
4. What is the magnetic contribution of the gabbro layer? Can the magnetic polarity structure of the lower crust be used to constrain cooling rates?

1. Is the lower crust formed by gabbro glaciers or sheeted sills?

There are two principal models for the accretion of the lower crust at fast spreading mid-ocean ridges (Fig. F11); the “Gabbro Glacier” model (Henstock et al., 1993; Phipps Morgan and Chen, 1993) and accretion by “Sheeted Sills” (e.g., Boudier et al., 1996; Kelemen et al., 1997; Korenaga and Kelemen, 1997; MacLeod and Yaouancq, 2000). Gabbro glacier models postulate that the entire lower crust is formed by ductile flow of solid material downward and outward from a single shallow axial magma chamber. In contrast, sheeted sill models are based on the crystallization of gabbro throughout the lower axial crust, with negligible downward flow of solid material (Kelemen et al., 1997).

High-level mafic cumulate rocks that balance the fractionated compositions of the dikes and lavas are a predicted consequence of both the gabbro glacier and sheeted sills modes of accretion, and cumulates should occur within a few hundred meters of the dike/gabbro boundary. Sampling the cumulate section through drilling will allow us to test the relative importance of these end-member mechanisms of crustal accretion. A gabbro glacier mode of crustal accretion will result in specific chemical and structural consequences for the lower oceanic crust that will be observable in drill core (Fig. F12). One would predict (1) that the upper plutonics and the lower crust have similar compositions and (2) that there will be increasing amounts of strain and subsolidus deformation in rocks with depth in the ocean crust.

Test 1.1: The gabbro glacier models predict that there will be no variation in cumulate composition (e.g., Mg#) with depth.

If all solidification of the lower crust takes place in the shallow melt lens, then there should be no vertical variation in the composition of the cumulates (e.g., Mg# of mafic phases). However, if the stacked sills model is correct, then we should see a gradual increase in the Mg# of the mafic phases with increasing depth in the section or a random vertical repartition of variable Mg# values. Studies of high-level plutonic rocks in Oman do show chemical trends with depth over a scale of kilometers (e.g., MacLeod and Yaouancq, 2000; S. Miyashita, pers. comm.), although small-scale (meters) chemical layering at the very base of the Oman crust is not well correlated with depth (Korenaga and Kelemen, 1998). Chemical layering in cumulate rocks should put constraints on melt migration and the size of magma lenses. Studies of cyclic variations in mineral trace element concentrations in Oman suggest the size of melt lenses is on the order of meters to hundreds of meters (Browning, 1984; Korenaga and Kelemen, 1997). Modeling the effects of melt flow through porous media such as a chemically layered crystal mush indicate that trace element correlations should be obliterated by melt-crystal reaction in hundreds to thousands of years (Korenaga and Kelemen, 1998). In Oman, chemical layering is well correlated for different elements and minerals, suggesting that the upwelling of melt through a crystal mush at the ridge axis cannot have occurred (Korenaga and Kelemen, 1998). These careful petrological tests have not been applied to rocks sampled from in situ ocean crust. The presence or absence of geochemical trends in whole-rock and mineral chemistry will place important boundaries on mechanisms of melt migration and magma emplacement in the lower oceanic crust.

Test 1.2: Gabbro glacier models predict increasing strain with depth.

Formation of the lower crust from a single high-level melt lens requires very large increases in strain with depth in the crust (Henstock et al., 1993; Phipps Morgan and Chen, 1993) that manifest as stronger shape and lattice fabrics. Such high strains have not been reported from rocks sampled in Hess Deep, but to date textural and structural measurements to estimate the extent of strain have not been employed on rocks from intact sections of fast spread ocean crust. If we find no evidence for increasing strain with depth, this would favor the multiple sills model. However, increasing strain with depth has been reported for the uppermost part of the foliated gabbro section of the Oman ophiolite (Nicolas et al., 2009), suggesting that subsidence does occur from the upper melt lens. Together with the evidence for sills, these observations may support a mixed model (Boudier et al., 1996).

2. Is the plutonic crust cooled by conduction or hydrothermal circulation?

The balance between conductive and hydrothermal cooling is key to understanding the thermal structure of the ocean crust, as well as for estimating the magnitude of hydrothermal chemical exchanges between the crust and oceans. Were the gabbros, particularly cumulate gabbros, cooled by conduction or hydrothermal fluids (Maclennan et al., 2005; Manning et al., 1996)? Were hydrothermal interactions pervasive or restricted to veins, and did alteration occur at black smoker or higher temperatures (350°–800°C)? Or did most of the hydrothermal interactions occur later at subgreenschist facies conditions (e.g., prehnite, clays) some distance away from the ridge? How do alteration effects relate to physical properties and the seismic layering of the crust? Simple gabbro glacier models suggest much slower rates of cooling for the lower crust ($\sim 0.02^\circ\text{C}/\text{y}$) than those required to match recent seismic tomographic models and compliance results from the EPR (Crawford and Webb, 2002; Crawford et al., 1999; Dunn et al., 2001). Multiple sills models require deep near-axis hydrothermal cooling and rapid cooling rates ($\sim 0.1^\circ\text{C}/\text{y}$), otherwise large-scale remelting of the lower crust will occur (Chen, 2001). However, deep hydrothermal cooling may also occur in some geometries of gabbro glacier models. Although the extent of hydrothermal cooling of the lower crust must be closely linked to the mode of magmatic accretion, quantifying these rates of cooling is a separate, important, and independently achievable objective.

Test 2.1: Are cooling rates much greater than expected from conductive heat transfer in the cumulates?

Recent petrological studies of the Oman ophiolite and Hole 504B have developed techniques for estimating the cooling rates of dikes and gabbros (Coogan et al., 2002, 2005a, 2005b). The Ca in olivine geospeedometer developed and refined by Coogan and others will allow the robust estimation of vertical variations in cooling rate that are sensitive enough to identify departures from conductive cooling profiles. Li measurements of coexisting igneous plagioclase and clinopyroxene provide an independent cooling geospeedometer (Coogan et al., 2005b).

Test 2.2: Quantify fluid evolution and fluxes through lower crust using trace elements and Sr and stable isotopic profiles.

Well-established petrologic and geochemical approaches will be used to characterize the nature and relative timing of hydrothermal exchange between seawater and the lower crust that complement the trace element cooling rate studies of magmatic minerals discussed above.

Mineral geothermometers, crosscutting vein mineral sequences coupled with trace element and strontium and stable isotopic measurements of whole-rock samples and mineral separates, can be used to establish the chemistry of fluids reacting with the lower crust (Gregory and Taylor, 1981; Bach et al., 2004; Coggon et al., 2004; Gillis, 1995; Manning et al., 1996; Teagle et al., 1998a, 1998b). By looking at ^{87}Sr and ^{18}O profiles away from hydrothermal mineral veins, we can establish the scale of fluid channeling in the lower crust (e.g., Bickle, 1992; Teagle and Bickle, 1993). The advection of seawater-derived tracers, particularly when whole-rock and mineral data are closely coupled, have proved useful for estimating time-integrated hydrothermal fluid fluxes (Bickle and Teagle, 1992; Gillis et al., 2005; Teagle et al., 2003).

3. What is the geological significance of the seismic Layer 2/3 boundary at Site 1256?

Understanding the seismic structure of the ocean crust requires the calibration of remotely obtained regional geophysical data against physical properties and petrological measurements of geological samples recovered from within deep ocean boreholes. Hole 504B remains the only site where the seismic Layer 2/3 boundary has been penetrated (e.g., Detrick et al., 1994). At that location, the change in seismic gradient clearly occurs within the dikes, and the Layer 2–3 transition reflects changes in bulk physical properties associated with an increased grade of hydrothermal alteration (albite + chlorite to amphibole + plagioclase). In Hole 1256D, gabbros have been recovered from crust clearly within seismic Layer 2 based on shipboard, wireline, and seismic refraction velocity measurements (Figs. F4, F7) (Swift et al., 2008). The depth of the Layer 2/3 boundary estimated during site survey seismic experiments at Site 1256 is between 1450 and 1750 mbsf. Drilling deeper at Site 1256 would provide a second test of the geological meaning of the seismic layering of the ocean crust, where the Layer 2–3 transition lies beneath the first appearance of gabbro.

4. What is the magnetic contribution of the gabbro layer? Can the magnetic polarity structure of the lower crust be used to constrain cooling rates?

Site 1256 was deliberately located ~5 km on the old side of the C5Cr–C5Bn magnetic reversal (Fig. F3). Preliminary interpretation of the downhole magnetic field indicates that the flow and dike section has reversed polarity. Interpretation of paleomagnetic samples has been severely hampered by drilling overprint. However, the downhole magnetic field is more diagnostic than analysis of samples for determining the average in situ magnetization of a particular crustal layer. Very preliminary modeling of the downhole field intensity suggests that the flow and dike layers contribute about

two-thirds of the amplitude of the marine magnetic anomalies measured at the sea surface, mostly from the thicker flow units. In addition to quantifying the contribution of gabbros to the sea-surface anomalies, magnetic measurements from a significantly deepened Hole 1256D could help determine whether the middle crust cools quickly by convection or slowly by conduction. The blocking temperature at which magnetization becomes stable over geologic time is ~400°C. The position of the site indicates that the Earth's field changed from reversed to normal polarity 50–80 k.y. after most dikes and the lower extrusives formed. End-member models for hydrothermal circulation therefore predict very different observations of the polarity structure of the middle and lower crust. Models for deep, young hydrothermal circulation (e.g., Maclennan et al., 2005) predict that the reversed polarity should continue to near the base of the crust. In contrast, models with young hydrothermal circulation largely restricted to the more porous upper crust (e.g., Henstock et al., 1993) predict that normal polarity should be encountered within a few hundred meters of the base of high-volume circulation, potentially within the penetration of an additional single drilling leg.

Operations plan

Background

Following ODP Leg 206, IODP Expeditions 309 and 312 made significant progress in recovering an intact section of the upper oceanic crust. Average rates of recovery and penetration are summarized in Figure **F13** and Table **T1**. The inverse relationship between spreading rate and depth to axial melt lenses has been confirmed, supporting the strategy of drilling in crust formed at a superfast spreading rate to achieve the first upper crustal penetration. Expedition 335 should deepen Hole 1256D sufficiently into plutonic rocks to obtain definitive answers to longstanding questions about the structure and composition of the oceanic crust and about mechanisms of crustal accretion.

The IODP Science Planning Committee requested in 2006 (SPC Consensus 0603-19) that the United States Implementing Organization (USIO) identify the operational requirements for further drilling in Hole 1256D. Texas A&M University (TAMU) Engineers from the USIO presented their operational plan to an audience of scientists and independent drilling engineers at the Mission Moho Workshop (Portland, Oregon, 7–9 September 2006) for technical review. There was consensus support for the plan pro-

posed, and the USIO report is available in the full report of the Mission Moho workshop (page 39; available online at www.iodp.org/mission-moho-workshop/).

Four deepening scenarios were considered:

1. Resume rotary core barrel (RCB) coring in Hole 1256D using large-volume (100–150 bbl) high-viscosity mud sweeps combined with frequent bit trips.
2. Enlarge the hole to 18½ inches to isolate the out-of-gauge section using 13¾ inch casing.
3. Forego 13¾ inch casing and enlarge the hole to 14¾ inches to isolate the out-of-gauge section using 10¾ inch casing.
4. Offset and start a new hole following the casing strategy employed during Leg 206.

Several key points were noted by USIO-TAMU and independent engineers at the Mission Moho Workshop. Hole 1256D is in excellent condition, and remedial engineering operations such as reaming and casing are premature. It is important to recognize that neither the offshore industry nor scientific ocean drilling operators have ever attempted to open up an existing deep basement hole to any significant depth in basalt and insert casing. Regardless of the casing strategy proposed (2 or 3), attempting to open any portion of Hole 1256D to accommodate casing would require significant new hardware and numerous pipe trips and would extend over several expeditions. Such operations would require unproven technology and would be extremely challenging with substantial risk of irreparable damage to Hole 1256D without any further coring or recovery. Approaches 2 and 3 are not viable options and are not considered further. Further deepening of Hole 1256D using large mud sweeps is the only strategy that begins with coring, is the most likely to return samples from deeper in the hole, and has the largest possibility of building on the tremendous success of previous deepening operations on Expedition 309 and 312 that employed proven drilling techniques.

Operations plan for Expedition 335

The operations plan for Expedition 335 is to resume RCB coring with frequent large-volume, high-viscosity mud sweeps. During Expeditions 309 and 312, large-volume mud sweeps were effective at clearing cuttings from the hole, but at the end of Phase 1 operations, mud stock depletion precluded implementation of this approach throughout the whole of Expedition 312. Following the recommendations of the

IODP Expedition 309/312 Operations Review Task Force, the *JOIDES Resolution* will be stocked with at least 60 T of sepiolite and attapulgite for use during Expedition 335. Assuming reasonable hole conditions and an average rate of penetration comparable to previous coring in this hole, TAMU engineers estimate that this approach should deepen Hole 1256D ~350 m within 39 days (Table T2; Fig. F14).

Before conditioning the hole for further deepening, an attempt will be made to acquire an equilibrium temperature profile and recover a water sample before the thermal structure of the crust is perturbed by cleaning and drilling operations (see next section). We will reenter the hole with a tricone drilling bit on a bit release and slowly descend past the zone around 900 mbsf that caused an obstruction during Expedition 312. If the hole is clear, we will withdraw the pipe, drop the bit on the seafloor, reenter to below the rat hole, and log the hole with the triple combination (triple combo) tool string, including the Modular Temperature Tool (MTT). If the wireline conditions are suitably benign, we will attempt to take a borehole water sample from near the bottom of the hole, where the temperature is anticipated to be close to the currently accepted limit of life, using the Water Sampling and Temperature Tool (WSTP).

Logging/downhole measurements strategy

Downhole logging will be an important complement to coring operations during Expedition 335 and will assist in the attainment of the scientific objectives by providing continuous in situ geophysical measurements of the drilled basalts, dikes, and gabbros that are commonly incompletely recovered. The logging program will establish the igneous stratigraphy, magmatic morphology, and variations in seawater-basaltic alteration as a function of depth, as well as allow direct correlation of wireline measurements with discrete laboratory measurements on the recovered core. In addition, core-log integration will be enhanced through the use of the DMT Digital Color 360° CoreScan system or a similar tool to digitally record the outer surface of all cores, as employed during Leg 206 and Expeditions 309 and 312. Wireline data will be used in conjunction with core images and structural and magnetic data to reorient veins, fractures, and other features back into the geographic reference frame.

Using the heat flow calculated based on temperature measurement in Hole 1256C (109 mW/m²), the temperature at the sediment/basement boundary (35°C) and appropriate thermal conductivities for lavas, dikes, and gabbroic rocks, we predict that the ambient temperature at 1700 mbsf in Hole 1256D should be ~100°–140°C, significantly cooler than was encountered in Hole 504B (~170°C) at these depths (Fig. F15).

Our operations schedule includes time for preliminary logging of Hole 1256D, which would require a dedicated round trip of the drill string, so that an equilibrium temperature profile and water sample can be recovered before the thermal structure of the crust is perturbed by drilling operations. We also expect to evaluate the diameter of the borehole with the triple combo tool string. In the unexpected case of significant fill and/or large changes in hole diameter, additional passes with the Formation MicroScanner (FMS) or the Ultrasonic Borehole Imager (UBI) may be made to evaluate the need for casing. A full suite of wireline logging tools will be deployed after the completion of drilling operations, following an order of operations used at the end of Expedition 312 and including a final temperature profile of the hole. The hole will be flushed with freshwater in order to improve the quality of resistivity measurements.

Precoring logging

1. Triple combo, including the MTT. The tool will be run into the hole after lowering the drill string to ~1000 mbsf to confirm that the hole is still open.
2. If conditions permit, water sampling with the WSTP.

Postcoring logging

The hole will be flushed with freshwater after completion of coring to reduce the electrical resistivity contrast between the borehole fluid and gabbroic wall rocks and enhance the quality of the images. This follows good practice recommended following wireline logging of gabbros during Leg 176 (Dick, Natland, Miller, et al., 1999) and undertaken during logging operations in IODP Hole U1309B (Blackman, Ildefonse, John, Ohara, Miller, MacLeod, et al., 2006).

1. Triple-combo, including the MTT and the High-Resolution Laterolog Array (HRLA) resistivity tool.
2. Vertical seismic profile with the Versatile Seismic Imager (VSI).
3. UBI.
4. FMS-sonic.
5. MTT, HRLA, and Hostile Environment Gamma Ray Sonde (HNGS) for a final temperature measurement.

The triple combo will be the first tool run to establish the hole conditions. The order of the other tool strings will be adjusted to ensure that the vertical seismic profile is acquired during daylight operations for marine mammal watch.

The characteristics of the tools are briefly described below.

Triple combo tool string

The triple combo consists of five probes:

1. The Accelerator Porosity Sonde (APS) uses an electronic neutron source to measure the porosity of the formation.
2. The Hostile Environment Litho-Density Sonde (HLDS) measures bulk density. It includes a caliper that will provide an assessment of the hole quality.
3. The HNGS measures the natural radioactivity of the formation and provides indications of Th, U, and K concentrations. These measurements can then be integrated with analytical studies to determine downhole geochemical variations in alteration.
4. The HRLA tool measures rock resistivity at two invasion depths.
5. The Lamont-Doherty Earth Observatory (LDEO) MTT tool will be attached at the bottom of the tool string to measure borehole temperature.

Formation MicroScanner/Dipole Sonic Imager tool string

The FMS-sonic tool string has two main components:

1. The Dipole Sonic Imager (DSI) records a full set of acoustic waveforms to measure the compressional and shear velocity of the formation (V_P and V_S). V_P can be combined with the density log to generate synthetic seismograms and provide high-resolution seismic/well integration.
2. The FMS consists of four orthogonal pads with 16 electrodes on each pad to record high-resolution microresistivity images of the borehole wall, which are useful for the identification of volcanic units and tectonic features (e.g., the presence of fractures and faults and their orientations). It includes a General Purpose Inclinometry Tool (GPIT) to orient the images and adjust them for tool motion. The HNGS is included in this tool string to allow correlation with other logging runs for establishing consistent depth estimates.

Ultrasonic Borehole Imager

The UBI measures the amplitude and transit time of an acoustic wave propagated into the formation. It provides high-resolution images with 100% borehole wall coverage, allowing the detection of small-scale fractures. The GPIT is deployed with the UBI and enables borehole images, fractures, and other structural features to be oriented. This can provide important information on the local stress field and borehole geometry

even within the casing. The HNGS is included in this tool string to allow correlation with other logging runs for establishing consistent depth estimates.

Verstile Seismic Imager

The VSI will be used to acquire a vertical seismic profile over the deeper section of the hole. It will be lowered in the borehole and anchored at 10–25 m depth intervals against the borehole wall to record the waves emitted by two 250 in³ Sercel G guns (Table T3) in parallel clusters suspended 2–7 m below sea surface. The result will be a complete depth-traveltime relationship to position the hole in the seismic stratigraphy as we target the Layer 2/3 boundary.

Risks and contingencies

Operational risks

The following operational risks were identified at the precruise meeting, based on past experience at ODP Holes 504B, 735B, and 1256D:

1. The hole is not accessible because of formation collapse and cannot be cleaned to the bottom of the hole.
2. Drilling equipment failure in the hole.
3. Wireline tools stuck in the hole.
4. Hole rectification operations that require specialist tools, equipment, or personnel not available during Expedition 335.

Weather-related risks are negligible and essentially avoided. Site 1256 has a 12 month weather window, and previous cruises to the site have not been affected by adverse conditions.

Risk responses

The above listed operational risks must be accepted and dealt with as they occur. The probability of the risks can be reduced to some degree by good operational practices. One of the reasons for success in Hole 1256D has been a prudent approach to operations, and to date there have been relatively few drilling equipment failures compared with other igneous crust holes. Aggressive drilling tactics have not been employed to increase penetration at the cost of core recovery. An appropriate suite of pre- and post-

coring wireline operations have been conducted so that maximum scientific information has been gained at this important legacy site. We will continue with this philosophy and attempt to both deepen Hole 1256D and keep the hole intact for future drilling. The drilling operations team, led by Ron Grout, will ensure that Expedition 335 will sail with the best possible arsenal of fishing tools (fishing jars and intensifiers) to recover or mill out drilling or logging equipment potentially lost in the hole. However, situations may arise that are impossible to anticipate and plan for.

The success of Expedition 335 will be judged based on the added depth of penetration in Hole 1256D and the rate of core recovery. The scientific ocean drilling community has invested significant time and resources to establish and drill Hole 1256D to 1507 mbsf. Hence, the stabilization and remediation of this important legacy hole will be the primary objective should we encounter operational difficulties. Expedition 335 will take as much time as is available to explore all approaches for cleaning and/or stabilizing Hole 1256D until there is agreement that available options are exhausted. We do not envisage that we could reach such a situation in <10 days.

We may conclude that further operations in the hole will jeopardize future attempts to resuscitate Hole 1256D. In that case, it would be prudent to wait for a return to Hole 1256D with an appropriate armory of hole cleaning/fishing tools and/or specialist personnel. Should this case arise, we will suspend cleaning/stabilization activities, complete science operations at the site (e.g., wireline logging), and then move on to our contingency program.

Contingency program

For the worst-case scenario, where operations in Hole 1256D must be abandoned for some reason, a contingency plan has been mandated by the Science Planning Committee (SPC) of the IODP Science Advisory Structure (SAS). The SPC instructions call for the *JOIDES Resolution* to transit to the Costa Rica Seismogenesis Project (CRISP) operational area and continue operations from where Expedition 334 left off (SPC Motion 0908-14; SPC Consensus 0908-16). The general scientific and operational objectives of the CRISP program can be found in the Expedition 334 Scientific Prospectus (Vannucchi et al., 2010). The detailed coring and/or logging activities for a potential contingency operation cannot be anticipated until Expedition 334 is concluded.

In case the contingency plan is executed, the following rules and protocols apply:

1. The priorities for CRISP contingency operations, to be finalized at a joint meeting of Co-Chief Scientists and Expedition Project Managers (EPMs) in port after Expedition 334, should favor coring of basement intervals in order to take advantage of the Expedition 335 scientific staff expertise. Expedition 335 will not include any sedimentologists or paleontologists.
2. Expedition 335 Superfast scientists will become Expedition 334 CRISP shipboard science party members by virtue of recovering cores and executing basic shipboard measurements. However, they will not incur any obligation to conduct postcruise research and publish for Expedition 334 unless they explicitly choose to do so with a proposed research title (and associated sample request) no later than the last day of the cruise. Such proposals and sample requests must be in consideration of the existing CRISP proposed postcruise projects and collaborative in nature as appropriate according to general IODP practices.
3. All CRISP science party members (i.e., those from Expeditions 334 and 335) will have moratorium access to Expedition 334 sample material. The postcruise moratorium is set no earlier than the end of Expedition 335. It could be delayed further if deemed necessary to allow all party members to adequately review and sample CRISP cores.

Sampling and data sharing strategy

Shipboard and shore-based researchers should refer to the IODP Sample, Data, and Obligations policy posted on the Web at www.iodp.org/program-policies/. This document outlines the policy for distributing IODP samples and data to research scientists, curators, and educators. The document also defines the obligations that sample and data recipients incur. The Sample Allocation Committee (SAC; composed of Co-Chief Scientists, Staff Scientist, and IODP curator on shore and curatorial representative on board ship) will work with the entire scientific party to formulate a formal expedition-specific sampling plan for shipboard and postcruise sampling.

Shipboard scientists are expected to submit sample requests (at smcs.iodp.org/) 3 months before the beginning of the expedition. Based on sample requests (shore based and shipboard) submitted by this deadline, the SAC will prepare a tentative sampling plan, which will be revised on the ship as dictated by recovery and cruise objectives. For the purpose of developing sample requests, participating scientists should expect to receive on the order of 25–100 samples of no more than 25 cm³. This is based on historic precedent from ODP and IODP designed to enable scientists to

complete a research program and meet the established publication deadlines. Post-cruise research projects that require more frequent sampling or larger sample volumes should be further justified in sample requests. The sampling plan will be subject to modification depending upon the actual material recovered and collaborations that may evolve between scientists during the expedition. Modification of the strategy during the expedition must be approved by the SAC.

The minimum permanent archive will be the standard archive half of each core. All sample frequencies and sizes must be justified on a scientific basis and will depend on core recovery, the full spectrum of other requests, and the cruise objectives. Some redundancy of measurement is unavoidable, but minimizing the duplication of measurements among the shipboard party and identified shore-based collaborators will be a factor in evaluating sample requests.

If some critical intervals are recovered (e.g., mineralization, veins, breccias, dike or glassy margins, thin gabbroic intervals, melt lenses, etc.), there may be considerable demand for samples from a limited amount of cored material. These intervals may require special handling, a higher sampling density, reduced sample size, or continuous core sampling by a single investigator. A sampling plan coordinated by the SAC may be required before critical intervals are sampled.

Following good practice established during Leg 206 and Expeditions 309/312, we strongly encourage collaboration among the shipboard and shore-based scientists so that the best use is made of the recovered core. Postcruise analytical programs should be coordinated to ensure that the full range of geochemical, isotopic, magnetic, and physical property studies are undertaken on a representative sample suite. Sampling all but the most critical intervals will take place on board the ship, and scientists are encouraged to develop collaborations before Expedition 335.

References

- Alt, J.C., Kinoshita, H., Stokking, L.B., et al., 1993. *Proc. ODP, Init. Repts.*, 148: College Station, TX (Ocean Drilling Program). [doi:10.2973/odp.proc.ir.148.1993](https://doi.org/10.2973/odp.proc.ir.148.1993)
- Alt, J.C., Laverne, C., Coggon, R.M., Teagle, D.A.H., Banerjee, N.R., Morgan, S., Smith-Duque, C.E., Harris, M., and Galli, L., 2010. Subsurface structure of a submarine hydrothermal system in ocean crust formed at the East Pacific Rise, ODP/IODP Site 1256. *Geochem., Geophys., Geosyst.*, 11(10):Q10010. [doi:10.1029/2010GC003144](https://doi.org/10.1029/2010GC003144)
- Alt, J.C., Laverne, C., Vanko, D.A., Tartarotti, P., Teagle, D.A.H., Bach, W., Zuleger, E., Erzinger, J., Honnorez, J., Pezard, P.A., Becker, K., Salisbury, M.H., and Wilkens, R.H., 1996. Hydrothermal alteration of a section of upper oceanic crust in the eastern equatorial Pacific: a synthesis of results from Site 504 (DSDP Legs 69, 70, and 83, and ODP Legs 111, 137, 140, and 148.) *In* Alt, J.C., Kinoshita, H., Stokking, L.B., and Michael, P.J. (Eds.), *Proc. ODP, Sci. Results*, 148: College Station, TX (Ocean Drilling Program), 417–434. [doi:10.2973/odp.proc.sr.148.159.1996](https://doi.org/10.2973/odp.proc.sr.148.159.1996)
- Anonymous, 1972. Penrose field conference on ophiolites. *Geotimes*, 17:24–25.
- Bach, W., Garrido, C.J., Paulick, H., Harvey, J., and Rosner, M., 2004. Seawater-peridotite interactions: first insights from ODP Leg 209, MAR 15°N. *Geochem., Geophys., Geosyst.*, 5(9):Q09F26. [doi:10.1029/2004GC000744](https://doi.org/10.1029/2004GC000744)
- Bédard, J.H., Sparks, R.S.J., Renner, R., Cheadle, M.J., and Hallworth, M.A., 1988. Peridotite sills and metasomatic gabbros in the eastern layered series of the Rhum complex. *J. Geol. Soc. (London, U. K.)*, 145(2):207–224. [doi:10.1144/gsjgs.145.2.0207](https://doi.org/10.1144/gsjgs.145.2.0207)
- Bickle, M.J., 1992. Transport mechanisms by fluid-flow in metamorphic rocks: oxygen and strontium decoupling in the Trois Seigneurs Massif: a consequence of kinetic dispersion? *Am. J. Sci.*, 292(5): 289–316. [doi:10.2475/ajs.292.5.289](https://doi.org/10.2475/ajs.292.5.289)
- Bickle, M.J., and Teagle, D.A.H., 1992. Strontium alteration in the Troodos ophiolite: implications for fluid fluxes and geochemical transport in mid-ocean ridge hydrothermal systems. *Earth Planet. Sci. Lett.*, 113(1–2):219–237. [doi:10.1016/0012-821X\(92\)90221-G](https://doi.org/10.1016/0012-821X(92)90221-G)
- Blackman, D.K., Ildefonse, B., John, B.E., Ohara, Y., Miller, D.J., MacLeod, C.J., and the Expedition 304/305 Scientists, 2006. *Proc IODP*, 304/305: College Station, TX (Integrated Ocean Drilling Program Management International, Inc.). [doi:10.2204/iodp.proc.304305.2006](https://doi.org/10.2204/iodp.proc.304305.2006)
- Boudier, F., Nicolas, A., and Ildefonse, B., 1996. Magma chambers in the Oman ophiolite: fed from the top and the bottom. *Earth Planet. Sci. Lett.*, 144(1–2):239–250. [doi:10.1016/0012-821X\(96\)00167-7](https://doi.org/10.1016/0012-821X(96)00167-7)
- Browning, P., 1984. Cryptic variation within the cumulate sequence of the Oman ophiolite: magma chamber depth and petrological implications. *In* Gass, I.G., Lippard, S.J., and Shelton, A.W. (Eds.), *Ophiolites and Oceanic Lithosphere*. Geol. Soc. Spec. Publ., 13(1):71–82. [doi:10.1144/GSL.SP.1984.013.01.07](https://doi.org/10.1144/GSL.SP.1984.013.01.07)
- Canales, J.P., Nedimovic, M.R., Kent, G.M., Carbotte, S.M., and Detrick, R.S., 2009. Seismic reflection images of a near-axis melt sill within the lower crust at the Juan de Fuca Ridge. *Nature (London, U. K.)*, 460(7251):89–93. [doi:10.1038/nature08095](https://doi.org/10.1038/nature08095)
- Cande, S.C., and Kent, D.V., 1995. Revised calibration of the geomagnetic polarity timescale for the Late Cretaceous and Cenozoic. *J. Geophys. Res., [Solid Earth]*, 100(B4):6093–6095. [doi:10.1029/94JB03098](https://doi.org/10.1029/94JB03098)
- Cannat, M., Karson, J.A., Miller, D.J., et al., 1995. *Proc. ODP, Init. Repts.*, 153: College Station, TX (Ocean Drilling Program). [doi:10.2973/odp.proc.ir.153.1995](https://doi.org/10.2973/odp.proc.ir.153.1995)

- Carbotte, S.M., Mutter, J.C., and Xu, L., 1997. Contribution of volcanism and tectonism to axial and flank morphology of the southern East Pacific Rise, 17°10'–17°40'S, from a study of Layer 2A geometry. *J. Geophys. Res., [Solid Earth]*, 102(B5):10165–10184. [doi:10.1029/96JB03910](https://doi.org/10.1029/96JB03910)
- Chen, Y.J., 2001. Thermal effects of gabbro accretion from a deeper second melt lens at the fast spreading East Pacific Rise. *J. Geophys. Res., [Solid Earth]*, 106(B5):8581–8588. [doi:10.1029/2000JB900420](https://doi.org/10.1029/2000JB900420)
- Coggon, R.M., Teagle, D.A.H., Cooper, M.J., and Vanko, D.A., 2004. Linking basement carbonate vein compositions to porewater geochemistry across the eastern flank of the Juan de Fuca Ridge, ODP Leg 168. *Earth Planet. Sci. Lett.*, 219(1–2):111–128. [doi:10.1016/S0012-821X\(03\)00697-6](https://doi.org/10.1016/S0012-821X(03)00697-6)
- Coogan, L.A., Hain, A., Stahl, S., and Chakraborty, S., 2005a. Experimental determination of the diffusion coefficient for calcium in olivine between 900°C and 1500°C. *Geochim. Cosmochim. Acta*, 69(14):3683–3694. [doi:10.1016/j.gca.2005.03.002](https://doi.org/10.1016/j.gca.2005.03.002)
- Coogan, L.A., Jenkin, G.R.T., and Wilson, R.N., 2002. Constraining the cooling rate of the lower oceanic crust: a new approach applied to the Oman ophiolite. *Earth Planet. Sci. Lett.*, 199(1–2):127–146. [doi:10.1016/S0012-821X\(02\)00554-X](https://doi.org/10.1016/S0012-821X(02)00554-X)
- Coogan, L.A., Kasemann, S.A., and Chakraborty, S., 2005b. Rates of hydrothermal cooling of new oceanic upper crust derived from lithium geospeedometry. *Earth Planet. Sci. Lett.*, 240(2):415–424. [doi:10.1016/j.epsl.2005.09.020](https://doi.org/10.1016/j.epsl.2005.09.020)
- Crawford, W.C., and Webb, S.C., 2002. Variations in the distribution of magma in the lower crust and at the Moho beneath the East Pacific Rise at 9°–10°N. *Earth Planet. Sci. Lett.*, 203(1):117–130. [doi:10.1016/S0012-821X\(02\)00831-2](https://doi.org/10.1016/S0012-821X(02)00831-2)
- Crawford, W.C., Webb, S.C., and Hildebrand, J.A., 1999. Constraints on melt in the lower crust and Moho at the East Pacific Rise, 9°48'N, using seafloor compliance measurements. *J. Geophys. Res., [Solid Earth]*, 104(B2):2923–2939. [doi:10.1029/1998JB900087](https://doi.org/10.1029/1998JB900087)
- Detrick, R., Collins, J., Stephen, R., and Swift, S., 1994. In situ evidence for the nature of the seismic Layer 2/3 boundary in oceanic crust. *Nature (London, U. K.)*, 370(6487):288–290. [doi:10.1038/370288a0](https://doi.org/10.1038/370288a0)
- Dick, H.J.B., Natland, J.H., Miller, D.J., et al., 1999. *Proc. ODP, Init. Repts.*, 176: College Station, TX (Ocean Drilling Program). [doi:10.2973/odp.proc.ir.176.1999](https://doi.org/10.2973/odp.proc.ir.176.1999)
- Dunn, R.A., Toomey, D.R., Detrick, R.S., and Wilcock, W.S.D., 2001. Continuous mantle melt supply beneath an overlapping spreading center on the East Pacific Rise. *Science*, 291(5510):1955–1958. [doi:10.1126/science.1057683](https://doi.org/10.1126/science.1057683)
- Expedition 309 Scientists, 2005. Superfast spreading rate crust 2: a complete in situ section of upper oceanic crust formed at a superfast spreading rate. *IODP Prel. Rept.*, 309. [doi:10.2204/iodp.pr.309.2005](https://doi.org/10.2204/iodp.pr.309.2005)
- Expedition 309 and 312 Scientists, 2006. Superfast spreading rate crust 3: a complete in situ section of upper oceanic crust formed at a superfast spreading rate. *IODP Prel. Rept.*, 312. [doi:10.2204/iodp.pr.312.2006](https://doi.org/10.2204/iodp.pr.312.2006)
- Farrell, J.W., Raffi, I., Janecek, T.R., Murray, D.W., Levitan, M., Dadey, K.A., Emeis, K.-C., Lyle, M., Flores, J.-A., and Hovan, S., 1995. Late Neogene sedimentation patterns in the eastern equatorial Pacific Ocean. In Piasias, N.G., Mayer, L.A., Janecek, T.R., Palmer-Julson, A., and van Andel, T.H. (Eds.), *Proc. ODP, Sci. Results*, 138: College Station, TX (Ocean Drilling Program), 717–756. [doi:10.2973/odp.proc.sr.138.143.1995](https://doi.org/10.2973/odp.proc.sr.138.143.1995)
- France, L., Ildefonse, B., and Koepke, J., 2009. Interactions between magma and the hydrothermal system in the Oman ophiolite and in IODP Hole 1256D: fossilisation of dynamic

- melt lens at fast spreading ridges. *Geochem., Geophys., Geosyst.*, 10(10):Q10O19. [doi:10.1029/2009GC002652](https://doi.org/10.1029/2009GC002652)
- Francheteau, J., Armijo, R., Cheminée, J.L., Hekinian, R., Lonsdale, P., and Blum, N., 1992. Dyke complex of the East Pacific Rise exposed in the walls of Hess Deep and the structure of the upper oceanic crust. *Earth Planet. Sci. Lett.*, 111(1):109–121. [doi:10.1016/0012-821X\(92\)90173-S](https://doi.org/10.1016/0012-821X(92)90173-S)
- Garmany, J., 1989. Accumulations of melt at the base of young oceanic crust. *Nature (London, U. K.)*, 340(6235):628–632. [doi:10.1038/340628a0](https://doi.org/10.1038/340628a0)
- Gillis, K., Mével, C., Allan, J., et al., 1993. *Proc. ODP, Init. Repts.*, 147: College Station, TX (Ocean Drilling Program). [doi:10.2973/odp.proc.ir.147.1993](https://doi.org/10.2973/odp.proc.ir.147.1993)
- Gillis, K.M., 1995. Controls on hydrothermal alteration in a section of fast-spreading oceanic crust. *Earth Planet. Sci. Lett.*, 134(3–4):473–489. [doi:10.1016/0012-821X\(95\)00137-2](https://doi.org/10.1016/0012-821X(95)00137-2)
- Gillis, K.M., Coogan, L.A., and Pedersen, R., 2005. Strontium isotope constraints on fluid flow in the upper oceanic crust at the East Pacific Rise. *Earth Planet. Sci. Lett.*, 232(1–2):83–94. [doi:10.1016/j.epsl.2005.01.008](https://doi.org/10.1016/j.epsl.2005.01.008)
- Gregory, R.T., and Taylor, H.P., Jr., 1981. An oxygen isotope profile in a section of Cretaceous oceanic crust, Samail ophiolite, Oman: evidence for $\delta^{18}\text{O}$ buffering of the oceans by deep (>5km) seawater-hydrothermal circulation at mid-ocean ridges. *J. Geophys. Res., [Solid Earth]*, 86(B4):2737–2755. [doi:10.1029/JB086iB04p02737](https://doi.org/10.1029/JB086iB04p02737)
- Hallenborg, E., Harding, A.J., Kent, G.M., and Wilson, D.S., 2003. Seismic structure of 15 Ma oceanic crust formed at an ultrafast spreading East Pacific Rise: evidence for kilometer-scale fracturing from dipping reflectors. *J. Geophys. Res., [Solid Earth]*, 108(B11):2532. [doi:10.1029/2003JB002400](https://doi.org/10.1029/2003JB002400)
- Henstock, T.J., Woods, A.W., and White, R.S., 1993. The accretion of oceanic crust by episodic sill intrusion. *J. Geophys. Res., [Solid Earth]*, 98(B3):4143–4161. [doi:10.1029/92JB02661](https://doi.org/10.1029/92JB02661)
- Karson, J.A., 2002. Geologic structure of the uppermost oceanic crust created at fast- to intermediate-rate spreading centers. *Annu. Rev. Earth Planet. Sci.*, 30:347–384. [doi:10.1146/annurev.earth.30.091201.141132](https://doi.org/10.1146/annurev.earth.30.091201.141132)
- Karson, J.A., Hurst, S.D., and Lonsdale, P., 1992. Tectonic rotations of dikes in fast-spread oceanic crust exposed near Hess Deep. *Geology*, 20(8):685–688. [doi:10.1130/0091-7613\(1992\)020<0685:TRODIF>2.3.CO;2](https://doi.org/10.1130/0091-7613(1992)020<0685:TRODIF>2.3.CO;2)
- Karson, J.A., Klein, E.M., Hurst, S.D., Lee, C.E., Rivizzigno, P.A., Curewitz, D., Morris, A.R., Miller, D.J., Varga, R.G., Christeson, G.L., Cushman, B., O'Neill, J.M., Brophy, J.G., Gillis, K.M., Stewart, M.A., and Sutton, A.L., 2002. Structure of uppermost fast-spread oceanic crust exposed at the Hess deep rift: implications for subaxial processes at the East Pacific Rise. *Geochem., Geophys., Geosyst.*, 3(1):1002. [doi:10.1029/2001GC000155](https://doi.org/10.1029/2001GC000155)
- Kelemen, P.B., and Aharonov, E., 1998. Periodic formation of magma fractures and generation of layered gabbros in the lower crust beneath oceanic spreading centers. In Buck, R., Delaney, P.T., Karson, J.A., and Lagabriele, Y. (Eds.), *Faulting and Magmatism at Mid-Ocean Ridges*. Geophys. Monogr., 106:267–289.
- Kelemen, P.B., Kikawa, E., Miller, D.J., et al., 2004. *Proc. ODP, Init. Repts.*, 209: College Station, TX (Ocean Drilling Program). [doi:10.2973/odp.proc.ir.209.2004](https://doi.org/10.2973/odp.proc.ir.209.2004)
- Kelemen, P.B., Koga, K., and Shimizu, N., 1997. Geochemistry of gabbro sills in the crust-mantle transition zone of the Oman ophiolite: implications for the origin of the oceanic lower crust. *Earth Planet. Sci. Lett.*, 146(3–4):475–488. [doi:10.1016/S0012-821X\(96\)00235-X](https://doi.org/10.1016/S0012-821X(96)00235-X)

- Koepke, J., Christie, D.M., Dziony, W., Holtz, F., Lattard, D., Maclennan, J., Park, S., Scheibner, B., Yamasaki, T., and Yamazaki, S., 2008. Petrography of the dike–gabbro transition at IDOP Site 1256 (equatorial Pacific): the evolution of the granoblastic dikes. *Geochem. Geophys. Geosyst.*, 9(7):Q07O09. doi:10.1029/2008GC001939
- Korenaga, J., and Kelemen, P.B., 1997. Origin of gabbro sills in the Moho transition zone of the Oman ophiolite: implications for magma transport in the oceanic lower crust. *J. Geophys. Res., [Solid Earth]*, 102(B12):27729–27749. doi:10.1029/97JB02604 doi:10.1029/97JB02604
- Korenaga, J., and Kelemen, P.B., 1998. Melt migration through the oceanic lower crust: a constraint from melt percolation modeling with finite solid diffusion. *Earth Planet. Sci. Lett.*, 156(1–2):1–11. doi:10.1016/S0012-821X(98)00004-1
- Langmuir, C.H., Bender, J.F., and Batiza, R., 1986. Petrological and tectonic segmentation of the East Pacific Rise, 5°30'N–14°30'N. *Nature (London, U. K.)*, 322(6078):422–429. doi:10.1038/322422a0
- Macdonald, K.C., Fox, P.J., Alexander, R.T., Pockalny, R., and Gente, P., 1996. Volcanic growth faults and the origin of Pacific abyssal hills. *Nature (London, U. K.)*, 380(6570):125–129. doi:10.1038/380125a0
- Macdonald, K.C., Haymon, R., and Shor, A., 1989. A 220 km² recently erupted lava field on the East Pacific Rise near lat 8°S. *Geology*, 17(3):212–216. doi:10.1130/0091-7613(1989)017<0212:AKRELF>2.3.CO;2
- Maclennan, J., Hulme, T., and Singh, S.C., 2005. Cooling of the lower oceanic crust. *Geology*, 33(5):357–366. doi:10.1130/G21207.1
- MacLeod, C.J., and Yaouancq, G., 2000. A fossil melt lens in the Oman ophiolite: implications for magma chamber processes at fast spreading ridges. *Earth Planet. Sci. Lett.*, 176(3–4):357–373. doi:10.1016/S0012-821X(00)00020-0
- Manning, C.E., Weston, P.E., and Mahon, K.I., 1996. Rapid high-temperature metamorphism of East Pacific Rise gabbros from Hess Deep. *Earth Planet. Sci. Lett.*, 144(1–2):123–132. doi:10.1016/0012-821X(96)00153-7
- Natland, J.H., and Dick, H.J.B., 1996. Melt migration through high-level gabbroic cumulates of the East Pacific Rise at Hess Deep: the origin of magma lenses and the deep crustal structure of fast-spreading ridges. In Mével, C., Gillis, K.M., Allan, J.F., and Meyer, P.S. (Eds.), *Proc. ODP, Sci. Results*, 147: College Station, TX (Ocean Drilling Program), 21–58. doi:10.2973/odp.proc.sr.147.002.1996
- Nedimovic, M.R., Carbotte, S.M., Harding, A.J., Detrick, R.S., Canales, J.P., Diebold, J.B., Kent, G.M., Tischer, M., and Babcock, J.M., 2005. Frozen magma lenses below the oceanic crust. *Nature (London, U. K.)*, 436(7054):1149–1152. doi:10.1038/nature03944
- Nicolas, A., Boudier, F., and France, L., 2009. Subsidence in magma chamber and the development of magmatic foliation in Oman ophiolite gabbros. *Earth Planet. Sci. Lett.*, 284(1–2):76–87. doi:10.1016/j.epsl.2009.04.012
- Nicolas, A., Boudier, F., and Ildefonse, B., 1996. Variable crustal thickness in the Oman ophiolite: implication for oceanic crust. *J. Geophys. Res., [Solid Earth]*, 101(B8):17941–17950. doi:10.1029/96JB00195
- Nicolas, A., Boudier, F., Ildefonse, B., and Ball, E., 2000. Accretion of Oman and United Arab Emirates ophiolite—discussion of a new structural map. *Mar. Geophys. Res.*, 21(3–4):147–180. doi:10.1023/A:1026769727917

- Pallister, J.S., and Hopson, C.A., 1981. Samail ophiolite plutonic suite: field relations, phase variation, cryptic variation and layering, and a model of a spreading ridge magma chamber. *J. Geophys. Res., [Solid Earth]*, 86(B4):2593–2644. doi:10.1029/JB086iB04p02593
- Park, S., Maclennan, J., Teagle, D., and Hauff, F., 2008. Did the Galápagos plume influence the ancient EPR?: a geochemical study of basaltic rocks from Hole 1256D. *Eos, Trans. Am. Geophys. Union*, 89(53)(Suppl.):V51F-2097. (Abstract) <http://www.agu.org/meetings/fm08/waisfm08.html>
- Parsons, B., and Sclater, J.G., 1977. An analysis of the variation of ocean floor bathymetry and heat flow with age. *J. Geophys. Res., [Solid Earth]*, 82:803–827. doi:10.1029/JB082i005p00803
- Phipps Morgan, J., and Chen, Y.J., 1993. The genesis of oceanic crust: magma injection, hydrothermal circulation, and crustal flow. *J. Geophys. Res., [Solid Earth]*, 98(B4):6283–6297. doi:10.1029/92JB02650
- Purdy, G.M., Kong, L.S.L., Christeson, G.L., and Solomon, S.C., 1992. Relationship between spreading rate and the seismic structure of mid-ocean ridges. *Nature (London, U. K.)*, 355(6363):815–817. doi:10.1038/355815a0
- Quick, J.E., and Denlinger, R.P., 1993. Ductile deformation and the origin of layered gabbro in ophiolites. *J. Geophys. Res., [Solid Earth]*, 98(B8):14015–14027. doi:10.1029/93JB00698
- Singh, S.C., Kent, G.M., Collier, J.S., Harding, A.J., and Orcutt, J.A., 1998. Melt to mush variations in crustal magma properties along the ridge crest at the southern East Pacific Rise. *Nature (London, U. K.)*, 394(6696):874–878. doi:10.1038/29740
- Sinton, J.M., and Detrick, R.S., 1992. Mid-ocean ridge magma chambers. *J. Geophys. Res., [Solid Earth]*, 97(B1):197–216. doi:10.1029/91JB02508
- Su, Y., and Langmuir, C.H., 2003. Global MORB chemistry compilation at segment scale [Ph.D. dissert.]. Columbia Univ., New York.
- Swift, S., Reichow, M., Tikku, A., Tominaga, M., and Gilbert, L., 2008. Velocity structure of upper ocean crust at Ocean Drilling Program Site 1256. *Geochem., Geophys., Geosyst.*, 9(10):Q10O13. doi:10.1029/2008GC002188
- Teagle, D.A.H., Alt, J.C., Chiba, H., Humphris, S.E., and Halliday, A.N., 1998a. Strontium and oxygen isotopic constraints on fluid mixing, alteration and mineralization in the TAG hydrothermal deposit. *Chem. Geol.*, 149(1–2):1–24. doi:10.1016/S0009-2541(98)00030-8
- Teagle, D.A.H., Alt, J.C., and Halliday, A.N., 1998b. Tracing the chemical evolution of fluids during hydrothermal recharge: constraints from anhydrite recovered in ODP Hole 504B. *Earth Planet. Sci. Lett.*, 155(3–4):167–182. doi:10.1016/S0012-821X(97)00209-4
- Teagle, D.A.H., Alt, J.C., Umino, S., Miyashita, S., Banerjee, N.R., Wilson, D.S., and Expedition 309/312 Scientists, 2006. *Proc. IODP*, 309/312: Washington, DC (Integrated Ocean Drilling Program Management International, Inc.). doi:10.2204/iodp.proc.309312.2006
- Teagle, D.A.H., and Bickle, M.J., 1993. The transport and exchange of geochemical tracers by fluid-rock interaction: application of theory to ancient and modern ocean crust. *RIDGE Events*, 4(2):5–9.
- Teagle, D.A.H., Bickle, M.J., and Alt, J.C., 2003. Recharge flux to ocean-ridge black smoker systems: a geochemical estimate from ODP Hole 504B. *Earth Planet. Sci. Lett.*, 210(1–2):81–89. doi:10.1016/S0012-821X(03)00126-2
- Teagle, D.A.H., Wilson, D.S., and Acton, G.D., 2004. The “road to the MoHole” four decades on: deep drilling at Site 1256. *Eos, Trans. Am. Geophys. Union*, 85(49):521. doi:10.1029/2004EO490002

- Tominaga, M., Teagle, D.A.H., Alt, J.C., and Umino, S., 2009. Determination of volcanostratigraphy of the oceanic crust formed at superfast spreading ridge: electrofacies analyses of ODP/IOPD Hole 1256D. *Geochem., Geophys., Geosyst.*, 10(1):Q01003. doi:10.1029/2008GC002143
- Tominaga, M., and Umino, S., 2010. Lava deposition history in ODP Hole 1256D: insights from log-based volcanostratigraphy. *Geochem., Geophys., Geosyst.*, 11(5):Q05003. doi:10.1029/2009GC002933
- Umino, S., Lipman, P.W., and Obata, S., 2000. Subaqueous lava flow lobes, observed on ROV *Kaiko* dives off Hawaii. *Geology*, 28(6):503–506. doi:10.1130/0091-7613(2000)28<503:SLFLOO>2.0.CO;2
- Vannucchi, P., Ujiie, K., and Gamage, K., 2010. Costa Rica seismogenesis project (CRISP): sampling and quantifying input to the seismogenic zone and fluid output. *IODP Sci. Prosp.*, 334. doi:10.2204/iodp.sp.334.2010
- White, S.M., Hayman, R.M., Fornari, D.J., Perfit, M.R., and Macdonald, K.C., 2002. Correlation between volcanic and tectonic segmentation of fast-spreading ridges: evidence from volcanic structures and lava flow morphology on the East Pacific Rise at 9°–10°N. *J. Geophys. Res., [Solid Earth]*, 107(B8):2173. doi:10.1029/2001JB000571
- White, S.M., Macdonald, K.C., and Hayman, R.M., 2000. Basaltic lava domes, lava lakes, and volcanic segmentation on the southern East Pacific Rise. *J. Geophys. Res., [Solid Earth]*, 105(B10):23519–23536. doi:10.1029/2000JB900248
- Wilson, D.S., 1996. Fastest known spreading on the Miocene Cocos–Pacific plate boundary. *Geophys. Res. Lett.*, 23(21):3003–3006. doi:10.1029/96GL02893
- Wilson, D.S., Hallenborg, E., Harding, A.J., and Kent, G.M., 2003. Data report: site survey results from Cruise EW9903. In Wilson, D.S., Teagle, D.A.H., Acton, G.D., *Proc. ODP, Init. Repts.*, 206: College Station, TX (Ocean Drilling Program), 1–49. doi:10.2973/odp.proc.ir.206.104.2003
- Wilson, D.S., Teagle, D.A.H., Acton, G.D., et al., 2003. *Proc. ODP, Init. Repts.*, 206: College Station, TX (Ocean Drilling Program). doi:10.2973/odp.proc.ir.206.2003
- Wilson, D.S., Teagle, D.A.H., Alt, J.C., Banerjee, N.R., Umino, S., Miyashita, S., Acton, G.D., Anma, R., Barr, S.R., Belghoul, A., Carlut, J., Christie, D.M., Coggon, R.M., Cooper, K.M., Cordier, C., Crispini, L., Durand, S.R., Einaudi, F., Galli, L., Gao, Y., Geldmacher, J., Gilbert, L.A., Hayman, N.W., Herrero-Bervera, E., Hirano, N., Holter, S., Ingle, S., Jiang, S., Kalberkamp, U. Kerneklian, M., Koepke, J., Laverne, C., Vasquez, H.L.L., MacLennan, J., Morgan, S., Neo, N., Nichols, H.J., Park, S.-H., Reichow, M.K., Sakuyama, T., Sano, T., Sandwell, R., Scheibner, B., Smith-Duque, C.E., Swift, S.A., Tartarotti, P., Tikku, A.A., Tominaga, M., Veloso, E.A., Yamasaki, T., Yamazaki, S., and Ziegler, C., 2006. Drilling to gabbro in intact ocean crust. *Science*, 312(5776):1016–1020. doi:10.1126/science.1126090

Expedition 335 Scientific Prospectus

Table T1. Rates of recovery and rate of penetration (ROP) in Hole 1256D.

Interval	Cored interval (m)	Average recovery (%)	Average ROP (m/h)
Hole 1256D, Cores 2R–234R	1231	37	1.2
Lavas and transition zone (Cores 2R–128R)	785	41	1.5
Upper dikes (Cores 129R–191R)	287	37	0.9
Granoblastic dikes (Cores 192R–213R)	63	7	0.5
Plutonic complex (Cores 214R–234R)	96	29	1.1
Gabbros (Cores 214R–224R and 230R–234R)	72	35	1.2

Expedition 335 Scientific Prospectus

Table T2. Expedition 335 operations plan and time estimate.

Site No.	Location (Latitude Longitude)	Sea Floor Depth (mbrf)	Operations Description	Transit (days)	Drilling Coring (days)	Log (days)
Balboa, Panama						
			Transit ~825 nmi from Balboa to Hole 1256D @ 10.5 kt	3.3		
Hole 1256D	06° 44.16' N 91° 56.06' W	3645	Locate hole, reenter, and advance to ~1200 mbsf with tricone bit and MBR to verify open hole			
			Pull out of the hole, drop bit, and reenter to ~ 230 mbsf		1.3	
			WL Temperature Measurement to ~1200 mbsf			0.5
			Recover drill string, change to tricone bit, reenter, clean out hole to 1507 mbsf			
			recover drillstring, and change to RCB bit		2.9	
			RCB core 1507 to 1857 m in basement (7 bits, 50 rot hr @ 1.0 m/hr) with 4.5 m cored intervals		31.6	
			WL Log from 1000 to 1857 mbsf with the Triple combo, FMS, VSI, UBI, and Temperature			2.7
			Transit ~825 nmi from Hole 1256D to Balboa Pilot @ 10.5 kt	3.3		
			Wait to begin transit of Panama, Canal	0.9		
			Transit ~44 nmi from Balboa Pilot to Colont @ 3.3 kt	0.5		
Colon, Panama				8.0	35.8	3.2
Subtotal On-Site Time:				39.0		
Total Operating Days:				47.0		
				51.0		

Table T3. Airgun source levels. (See table notes.)

Source	Specification
Energy source	One or two 250 in ³ G airguns
Source output (downward) (1 x 250 in ³)	0-pk* is 3.1 bar-m (229.8 dB re 1 μPa·m) [‡] pk-pk [†] is 6.4 bar-m (236.2 dB re 1 μPa·m _{p-p})
Source output (downward) (2 x 250 in ³)	0-pk is 5.2 bar-m (234.3 dB re 1 μPa·m) _p pk-pk is 10.8 bar-m (240.7 dB re 1 μPa·m _{p-p})
Deployment depth of energy source (m)	2-7
Air discharge volume (in ³)	250 or 500
Dominant frequency components (Hz)	0-256

Notes: * = 0-pk = peak energy, † = pk-pk = peak to peak energy, ‡ = the source level is a measure of the effective sound pressure at a given distance from the source array, relative to a reference value. It is commonly expressed in decibels at 1 m from the source relative to μPascal-m, or dB re 1 μPa-m.

Figure F1. Age map of the Cocos plate and corresponding regions of the Pacific plate (Wilson, Teagle, Acton, et al., 2003). Isochrons at 5 m.y. intervals have been converted from magnetic anomaly identifications according to the timescale of Cande and Kent (1995). Selected DSDP and ODP sites that reached basement are indicated. The wide spacing of 10–20 m.y. isochrons to the south reflects the extremely fast (200–230 mm/y) full spreading rate. The dashed box shows the location of Figure F3A. FZ = fracture zone.

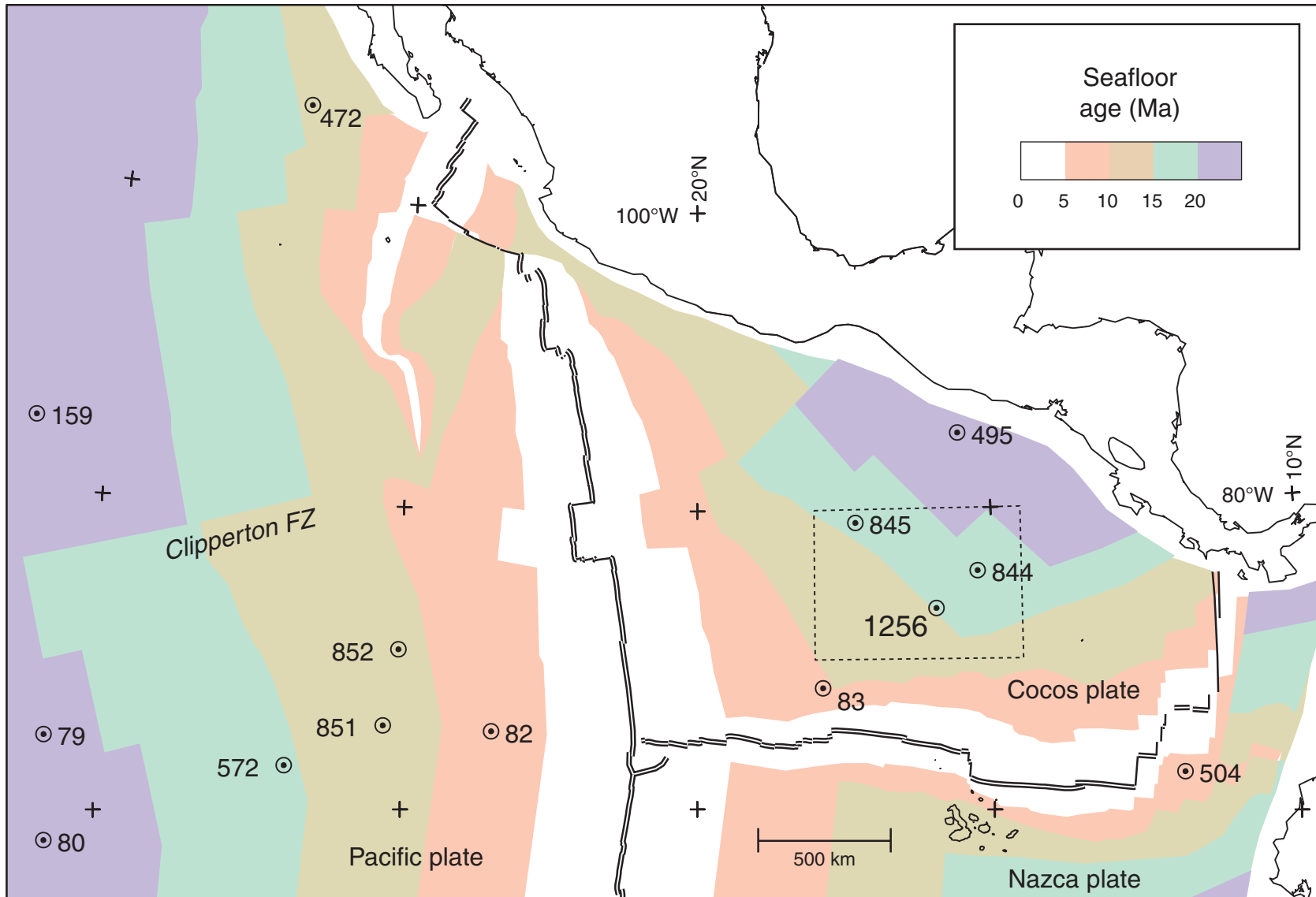


Figure F2. Depth to axial low-velocity zone plotted against spreading rate (Carbotte et al., 1997; Purdy et al., 1992). Depth versus spreading rate predictions from two models of Phipps Morgan and Chen (1993) are shown, extrapolated subjectively to 200 mm/y. Penetration to date in Holes 504B and 1256D is shown, with the depth at which gabbros were intersected indicated by the red box. Following core descriptions a thickness of ~300 m of off-axis lavas is shown for Hole 1256D and assumed for Hole 504B. EPR = East Pacific Rise, JdF = Juan de Fuca Ridge, Lau = Valu Fa Ridge in Lau Basin, CRR = Costa Rica Rift, MAR = Mid-Atlantic Ridge.

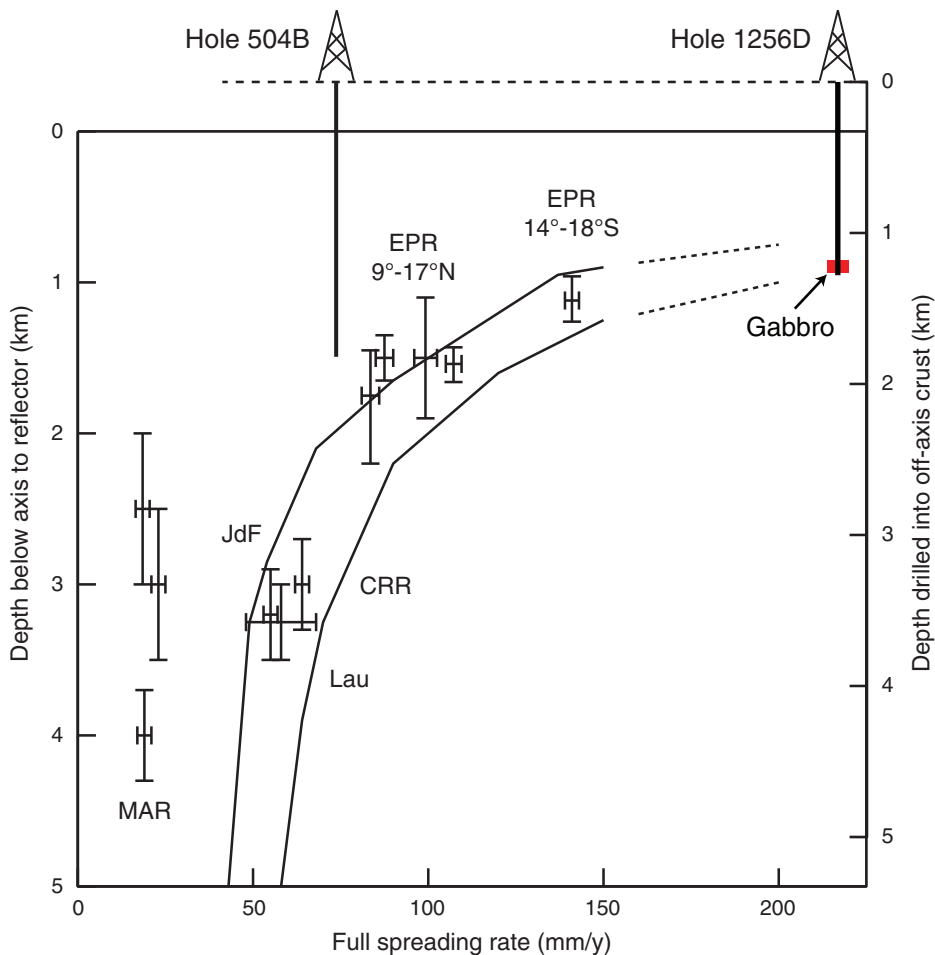


Figure F3. A. Details of isochrons inferred from magnetic anomalies near Site 1256. Shading shows normal magnetic polarity based on digitized reversal boundaries (small circles, after Wilson, 1996). Bold line shows location of Guatemala Basin multichannel seismic (MCS) track lines from the site survey Cruise EW9903 conducted in March–April 1999 (Wilson et al., 2003). Anomaly ages: 5A = ~12 Ma, 5B = 15 Ma, and 5D = ~17 Ma. **B.** Bathymetry and site survey track map for Site 1256 (proposed Site GUATB-03C). Abyssal hill relief of up to 100 m is apparent in the southwest part of the area; relief to the northeast is lower and less organized. Line numbers 21–28 identify MCS lines from the site survey.

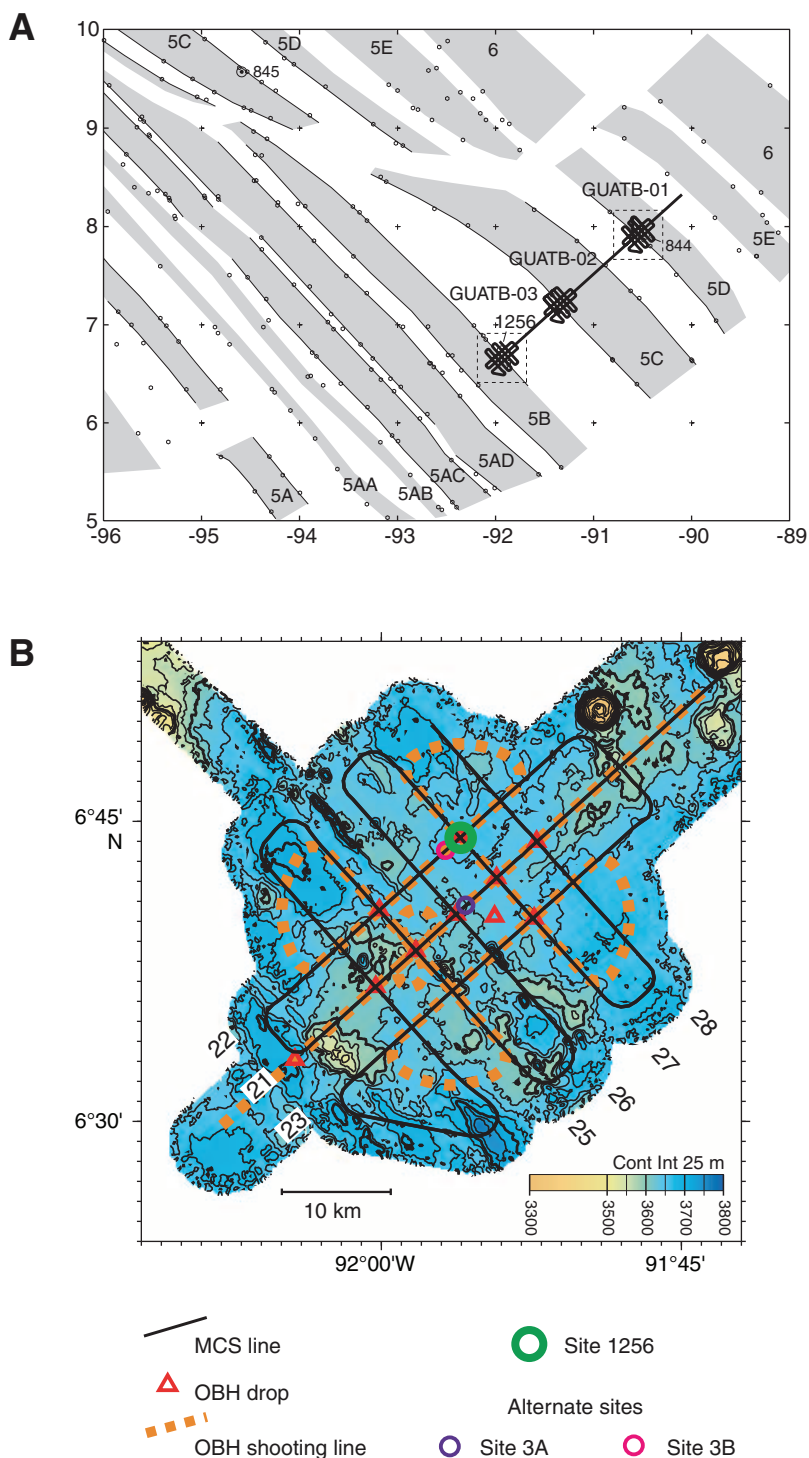


Figure F4. Summary lithostratigraphic column of the basement drilled to date at Site 1256 showing recovery; major lithologies; downcore index alteration mineral distribution (thick lines = abundant; thin lines = rare); downcore distribution of Mg# (where $Mg\# = 100 \times Mg/[Mg + 0.9 \times Fe]$) atomic ratio; symbols as in Fig. F10); and seismic velocity measured on discrete samples, wireline tools, and seismic refraction (from Wilson et al., 2003). Heavy red and orange lines show the inversion of traveltimes from Leg 206 and Expedition 312 vertical seismic profiles (VSP), respectively (Swift et al., 2008).

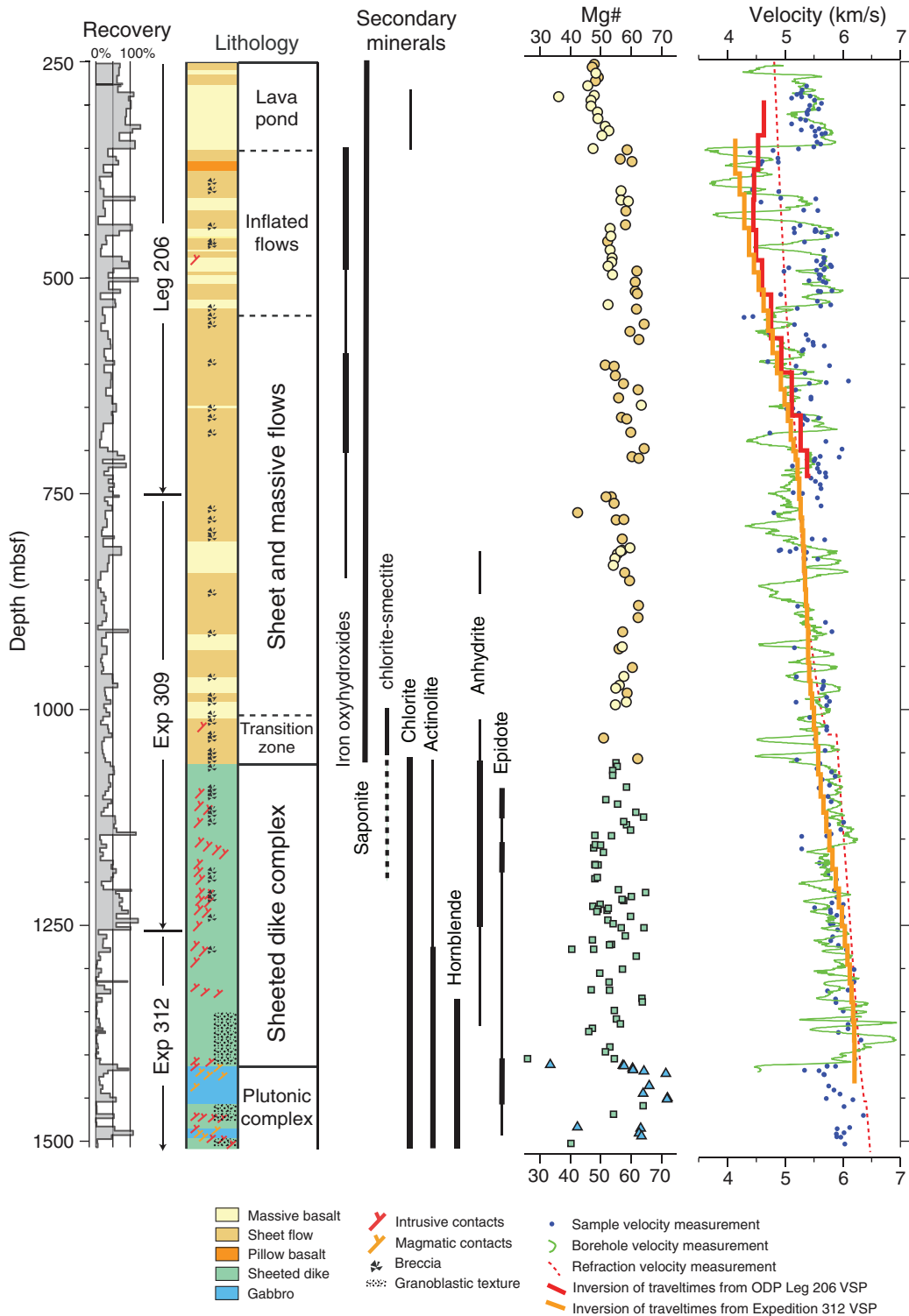


Figure F5. Reconstruction of Site 1256 and vicinity at 14 Ma, ~1 m.y. after formation of the site at the East Pacific Rise. Positions and plate velocities (arrows labeled in millimeters per year) are relative to the Antarctic plate, which is reasonably fixed relative to the spin axis and hotspots. Reconstructed positions of mapped magnetic Anomalies 5B, 5C, and 6 (ages 15–20 Ma) and existing DSDP/ODP drill sites are shown by shaded bars and circles, respectively.

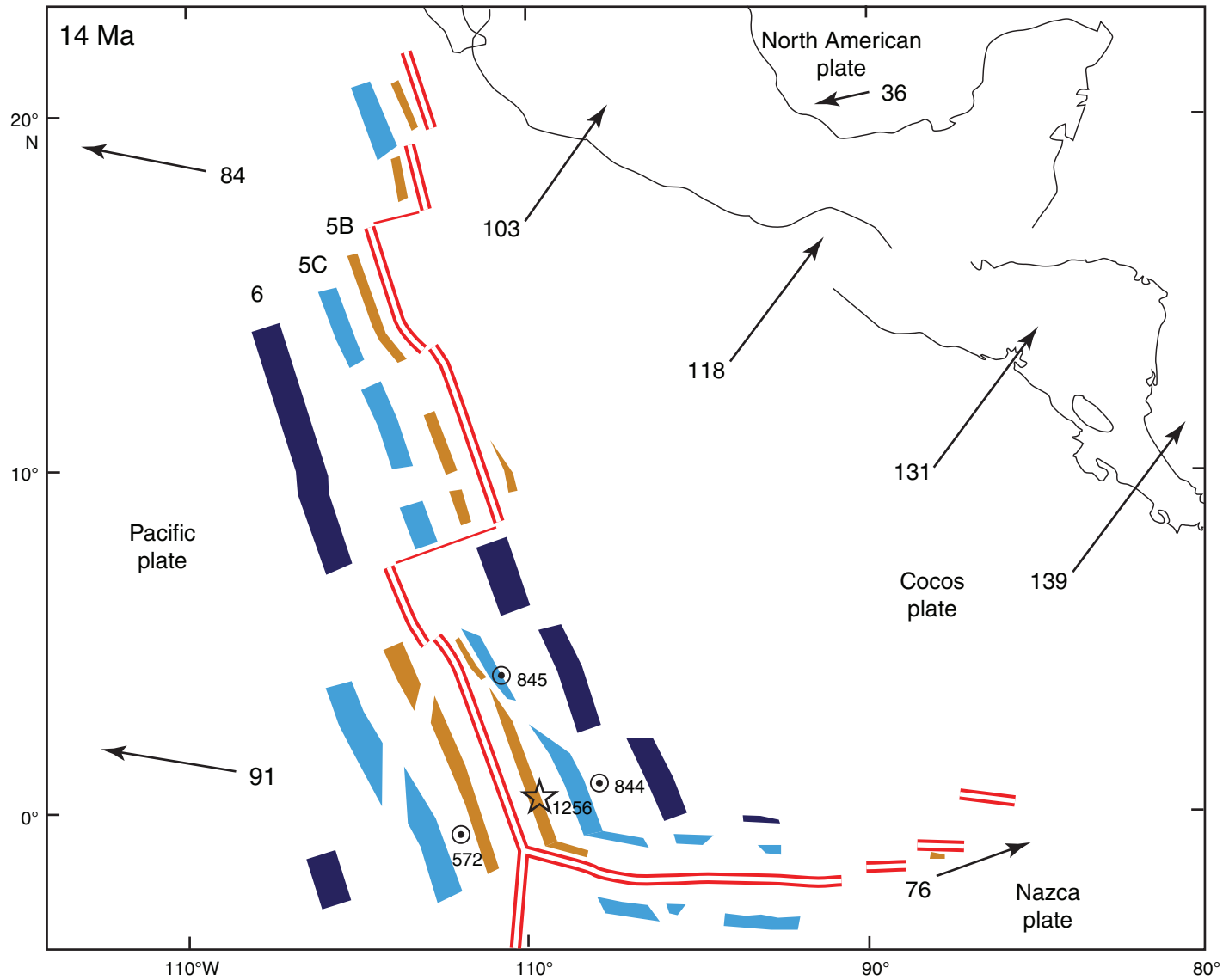


Figure F6. Site survey MCS data (Hallenborg et al., 2003) from the lines that cross at Site 1256, with penetration as of the end of Expedition 309 scaled approximately to traveltimes. Distances are in km. Horizontal reflectors in the upper basement to traveltimes of 5.5 s appear to result from contrasts between lava flow sequences, corresponding to depths of at least 800 meters subbasement.

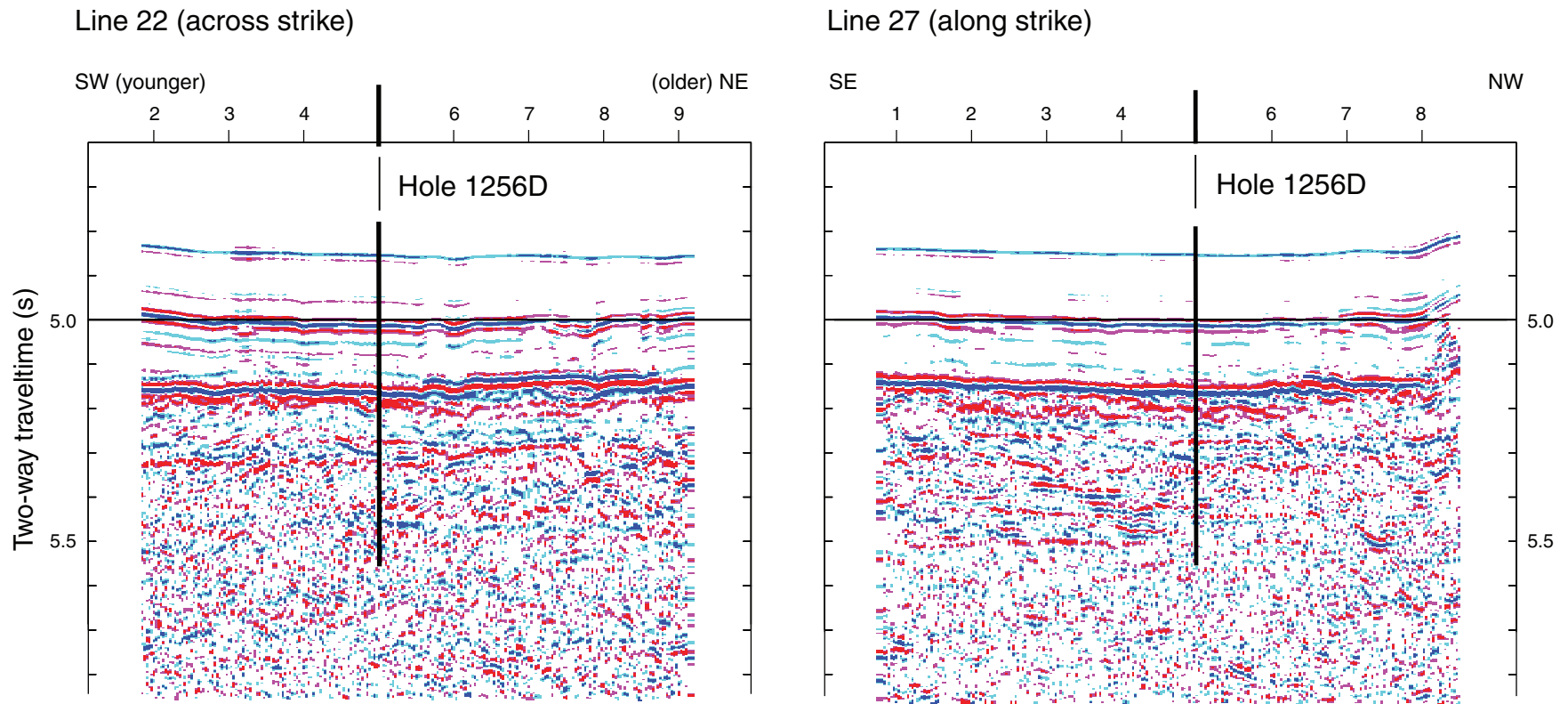


Figure F7. One-dimensional velocity model based on inversion of refraction data, Site 1256. At shallow depths, separate inversions were performed on northeast and southwest data subsets, with slightly faster velocities found to the northeast where abyssal hill topography is very subdued. The Layer 2/3 boundary is present in the depth range 1.2–1.5 km. The velocity model of Detrick et al. (1994) for Site 504, also based on ocean bottom hydrophone refraction, is shown for comparison. Apparent differences are dominated by differences in the inversion techniques, but the differences at 1.3–1.7 km may be barely above uncertainty.

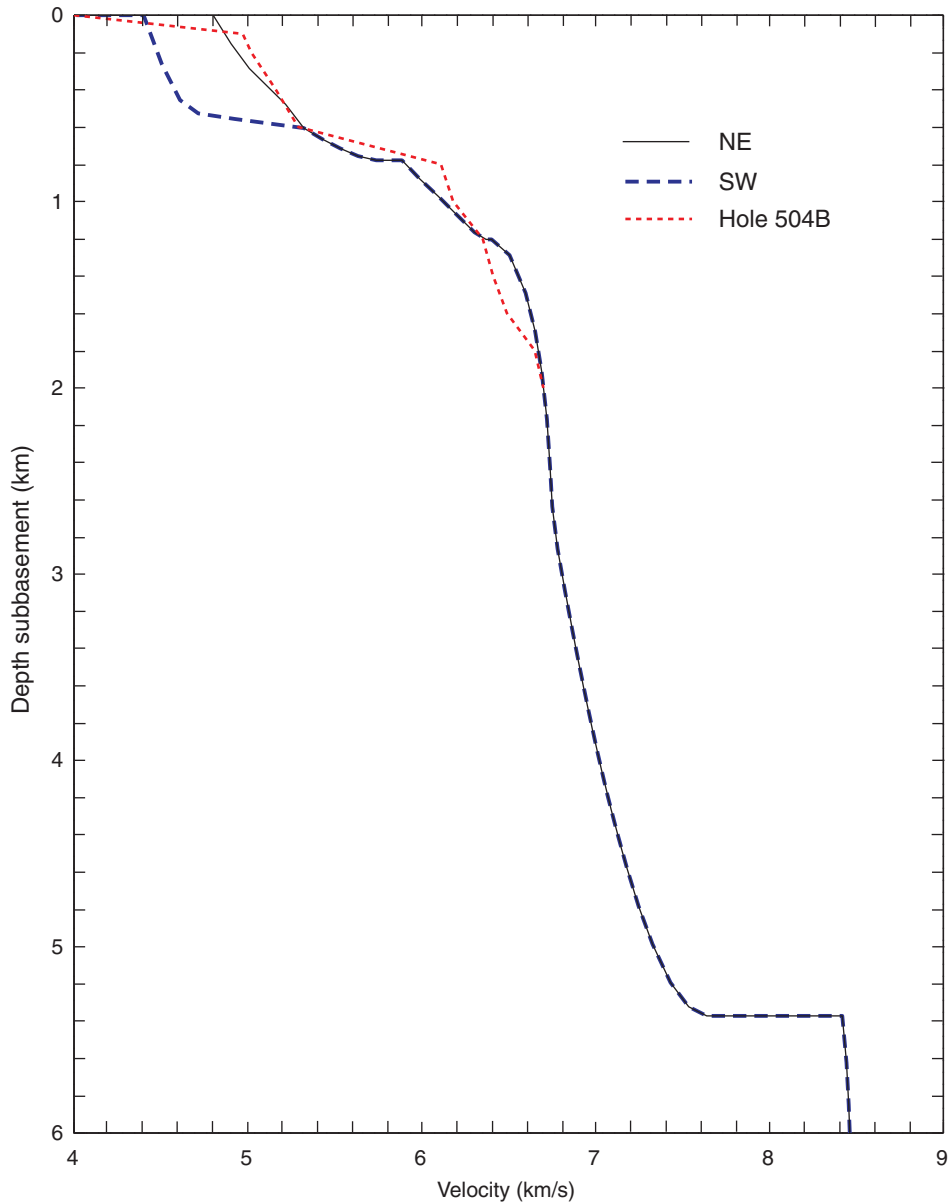


Figure F8. A. Contour map of seismic *P*-wave velocity at the top of basement, based on tomographic inversion of seismic refraction data (Alistair Harding, in prep.). The low-velocity area southwest of the center may reflect pillow lavas or other porous formation. The high-velocity area extending southeast from Site 1256 may reflect the extent of the ponded lava sequence drilled at the top of Site 1256. OBH = ocean borehole seismometer. **B.** Geological sketch map of the Site 1256 area (GUATB-03) showing bathymetry, alternate site locations, and selected top-of-basement velocity contours from A. The larger velocity contour line partially encloses velocity >4.82 km/s, which we interpret as a plausible proxy for the presence of thick ponded lava flows, as encountered at Site 1256. The smaller contour encloses velocities <4.60 km/s, possibly reflecting a greater portion of pillow lavas than elsewhere in the region. Alternate reentry sites 3D and 3E are 0.5–1.0 km from Site 1256.

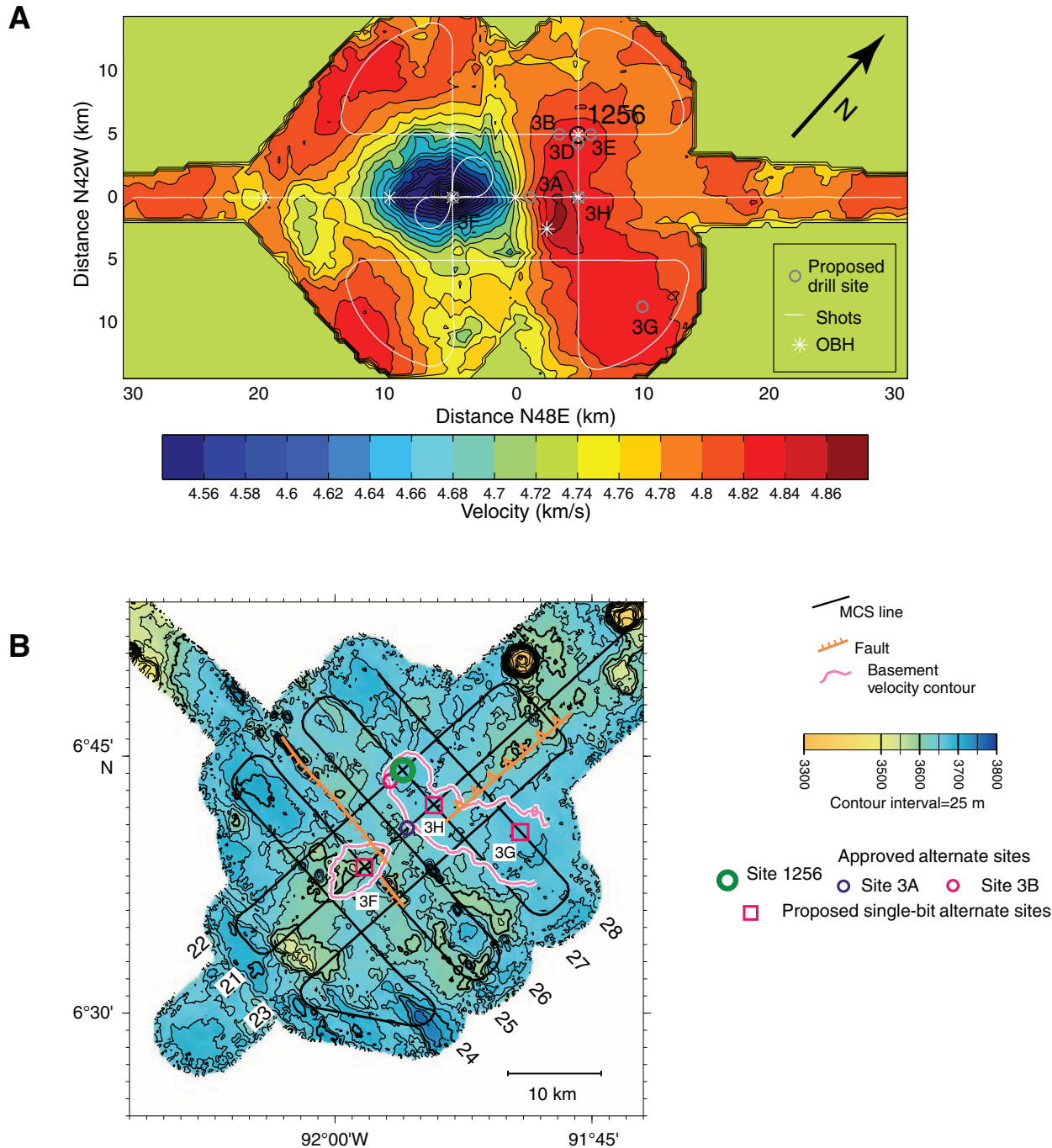


Figure F9. **A.** Schematic lithostratigraphic section of the plutonic complex from the lower portion of Hole 1256D with representative photographs of key samples. The distribution of rock types is expanded proportionately in zones of incomplete recovery. Felsic plutonic rocks include quartz-rich oxide diorite and trondjemite. OPX = orthopyroxene. **B.** Photomicrograph of a dike completely recrystallized to a granoblastic association of equant secondary plagioclase, clinopyroxene, magnetite, and ilmenite. Some granoblastic dikes have minor orthopyroxene. **C.** The dike/gabbro boundary! Medium-grained oxide gabbro is intruded into granoblastically recrystallized dike along an irregular, moderately dipping contact. The gabbro is strongly hydrothermally altered. **D.** Quartz-rich oxide diorite strongly altered to actinolitic hornblende, secondary plagioclase, epidote, and chlorite. Epidote occurs in ~5 mm clots in the finer grained leucocratic portions of the rock. **E.** Disseminated oxide gabbro with patchy texture and centimeter-scale dark ophitically intergrown clinopyroxene and plagioclase patches separated by irregular, more highly altered leucocratic zones. **F.** Medium-grained strongly hydrothermally altered gabbro. The sample is cut by several chlorite + actinolite veins with light gray halos. Plagioclase is replaced by secondary plagioclase and clinopyroxene by amphibole. **G.** Clast of partially resorbed dike within gabbro. ([Figure shown on next page.](#))

Figure F9 continued. (Caption shown on previous page.)

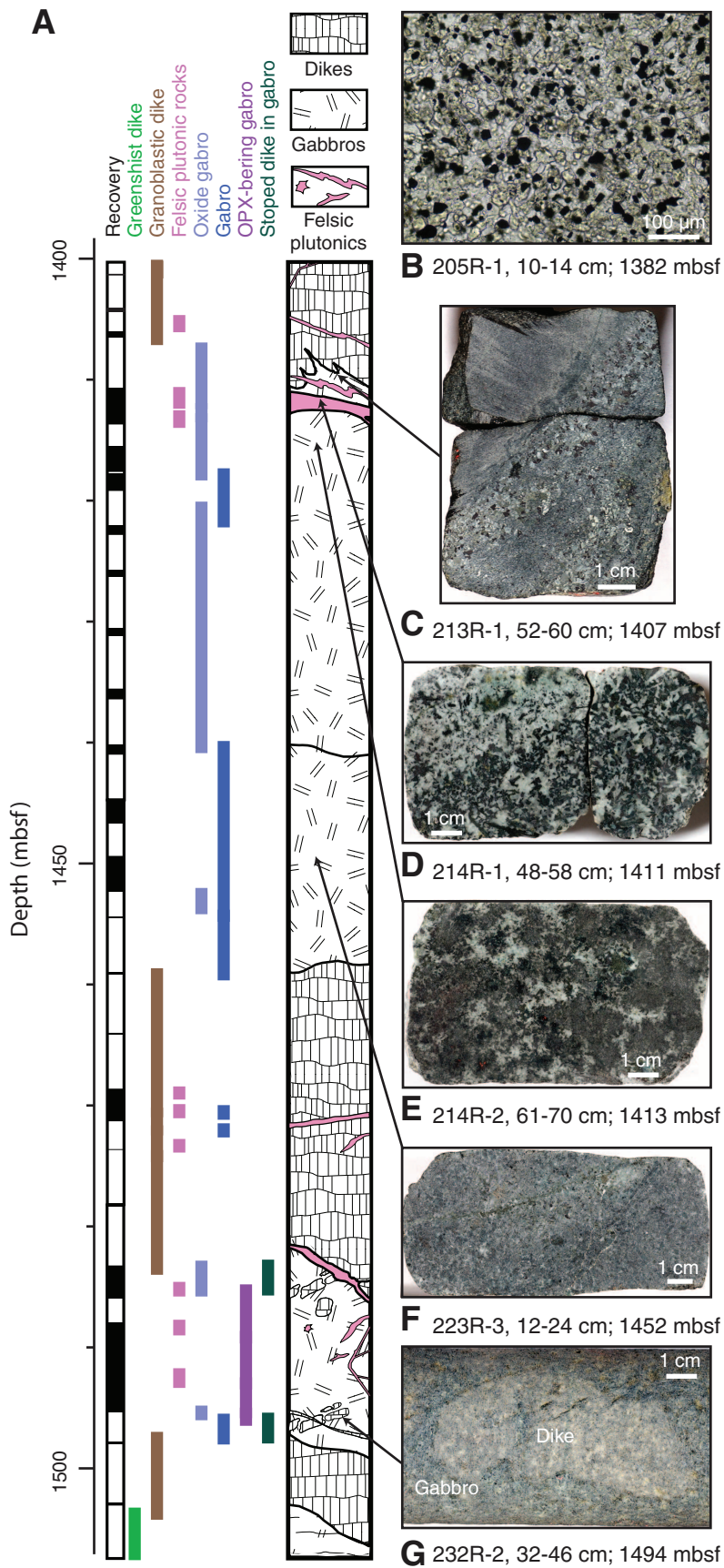


Figure F10. FeOT (total Fe expressed as FeO) vs. MgO for the basement at Site 1256, compared with analyses of northern East Pacific Rise (EPR) (outline, Langmuir et al., 1986). Dashed lines show constant Mg#. Possible primary mantle melt compositions should have Mg# of 70–78 and MgO of 9–14 wt%. All flows and dikes and most gabbros are too evolved to be candidates for primary magmas.

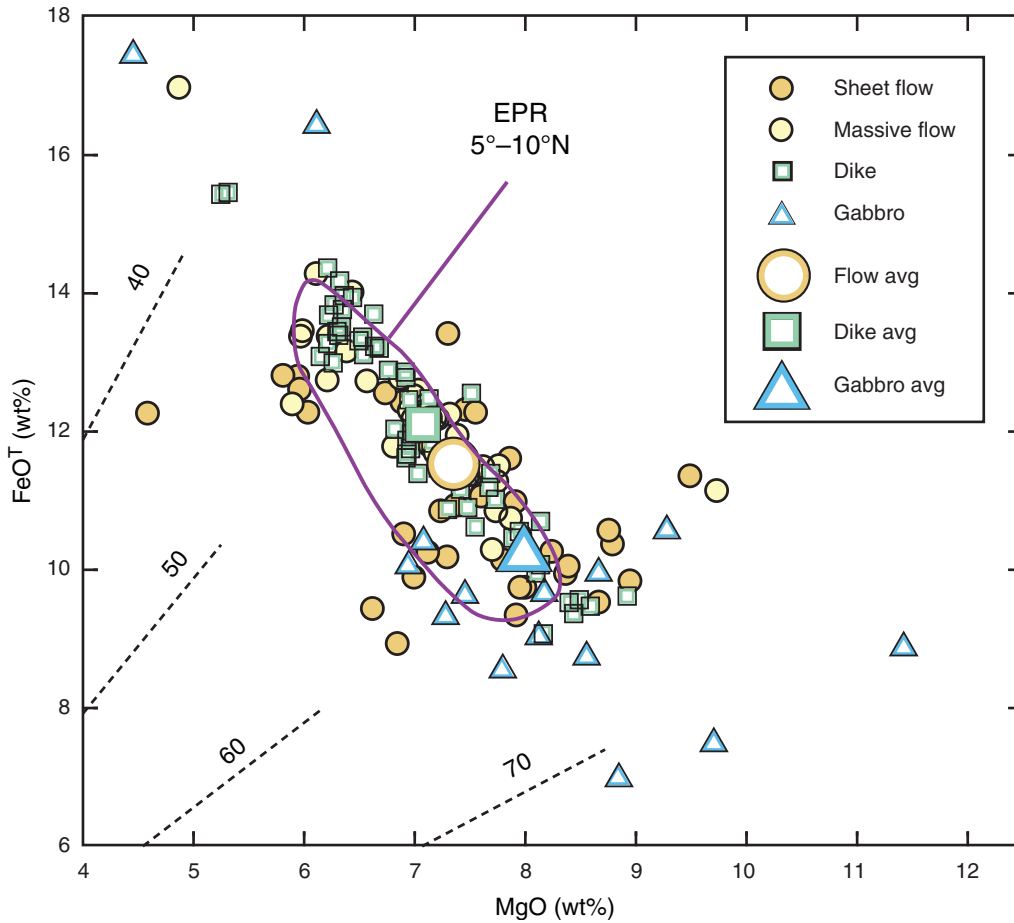


Figure F11. Schematic drawings of crustal accretion models (modified from Korenaga and Kelemen, 1998) under discussion with regards to Site 1256. **A.** Gabbro glacier ductile flow model (e.g., Henstock et al., 1993; Phipps Morgan and Chen, 1993; Quick and Denlinger, 1993). Ductile flow down and outward from a high-level axial magma chamber constructs the lower crust. **B.** A hybrid model of ductile flow with sill intrusions (e.g., Boudier et al., 1996). **C.** “Sheeted” or “stacked” sill model of in situ formation of the lower crust by on-axis sill intrusions (e.g., Bédard et al., 1988; Kelemen and Aharonov, 1998; Kelemen et al., 1997; MacLeod and Yoauancq, 2000).

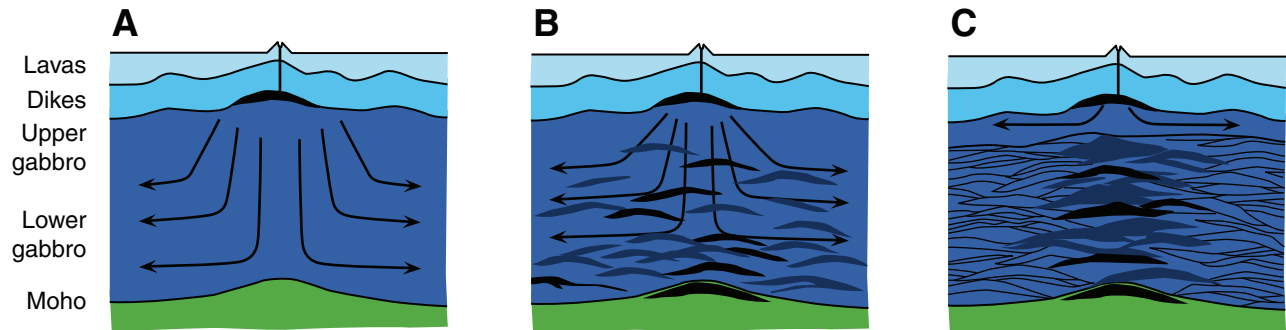


Figure F12. Schematic relative variations in the general trends of latent heat release, bulk Mg#, strain rate, cooling rate, hydrothermal fluid flux, fluid temperature, and intensity of high-temperature (HT) alteration with depth predicted by end-member “gabbro glacier” (with mainly conductive cooling of the lower crust) and “sheeted sill” (with convective cooling of the lower crust) models of crustal accretion (original figure by Rosalind Coggon). These trends are under discussion with regards to Site 1256.

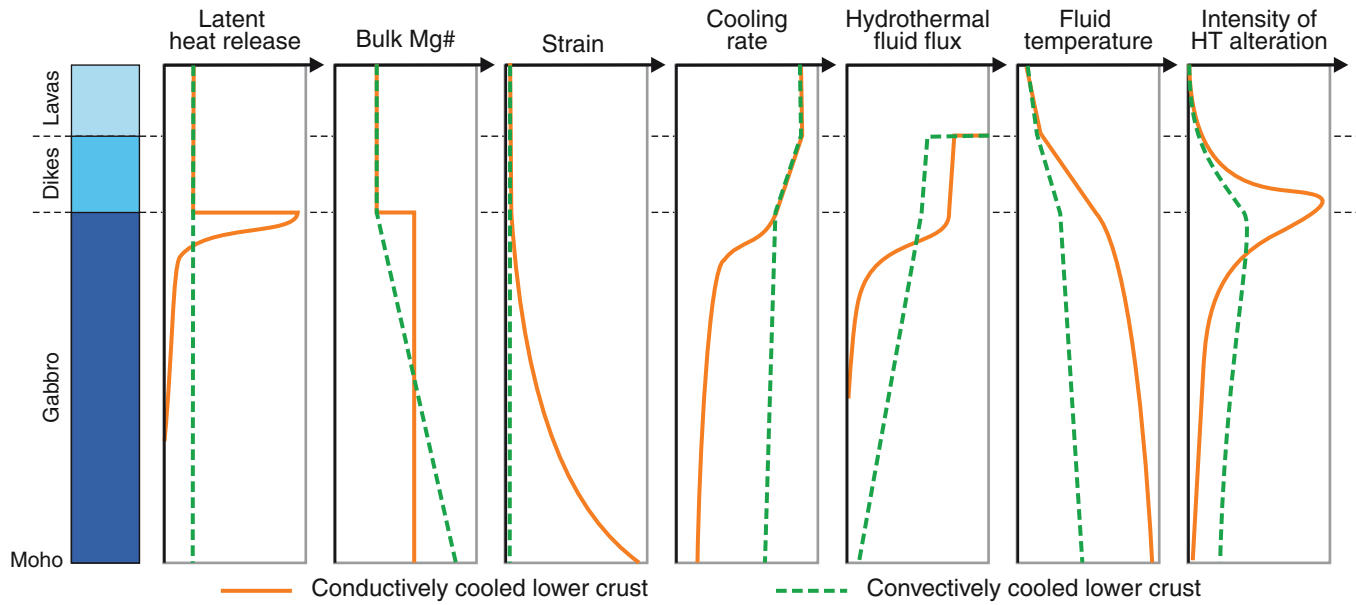


Figure F13. Average rates of core recovery and penetration for drilling in Hole 1256D. Note the improvement in both parameters in gabbroic rocks back to near average rates for the entire hole (~36% recovery; ~1.2 m/h penetration rate). Recovery was very low and penetration excruciatingly slow in the granoblastic dikes. ROP = rate of penetration.

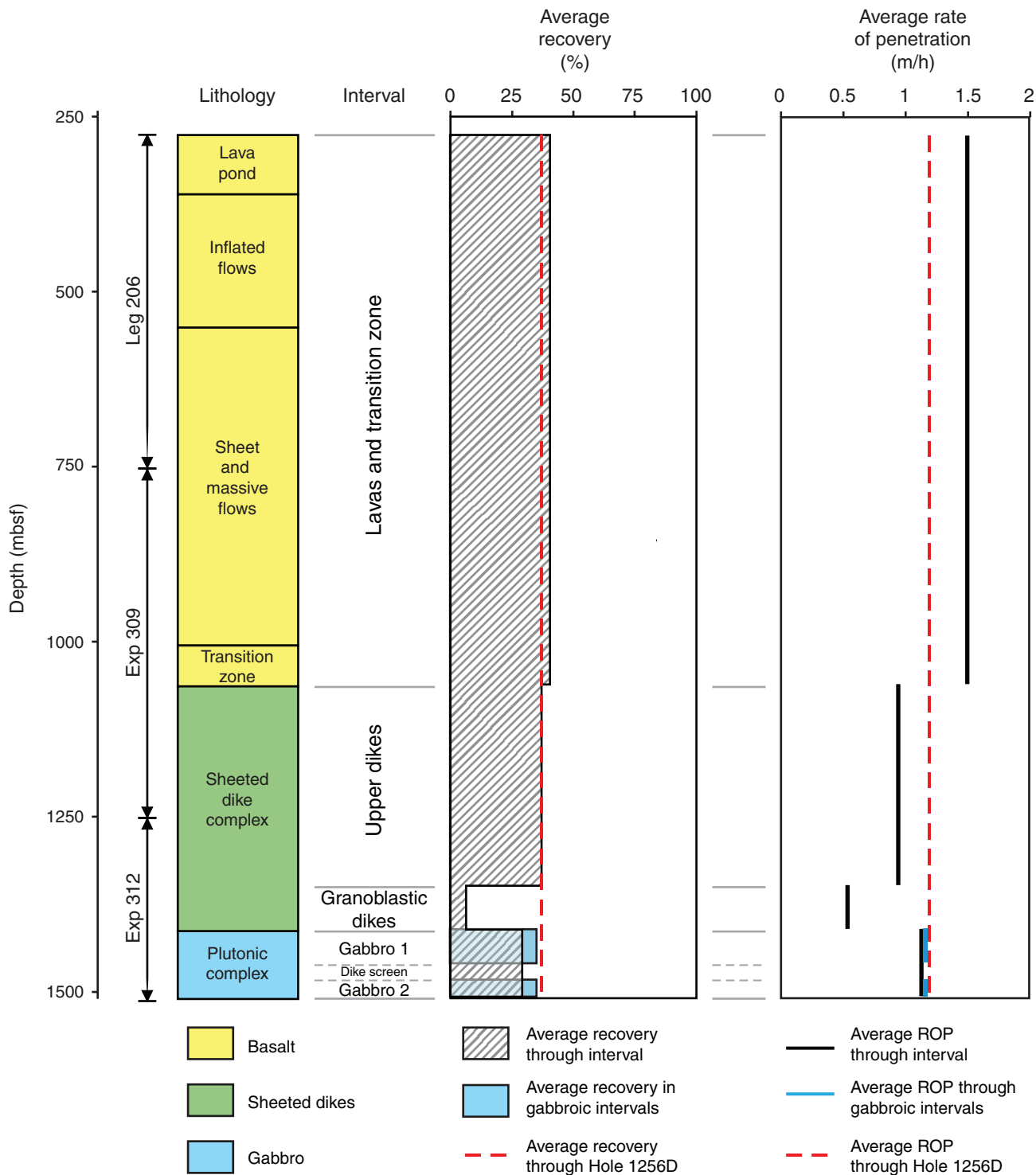


Figure F14. Proposed operations schedule in Hole 1256D during IODP Expedition 335, Superfast Spreading Rate Crust 4. Heavy red line shows our estimate of progress in Hole 1256D for Expedition 335 as scheduled for 51 days with 31.6 days of RCB coring. Transit, preparation, and wireline logging times based on previous operations in Hole 1256D. Assuming good drilling conditions, Hole 1256D should be deepened through the dike-gabbro transition zone and varitextured gabbros (coarse-grained melts of the same composition as the upper crust) and have a strong chance of penetrating down into cumulate gabbros. Upper crustal stratigraphy defined by drilling in Hole 1256D (Wilson et al., 2003, 2006; Teagle et al., 2006). Plutonic stratigraphy predicted from observations of the Oman ophiolite. Gray transparent boxes indicate uncertainty in predictions. Port = port call; Trans = transit; WL = downhole wireline experiments.

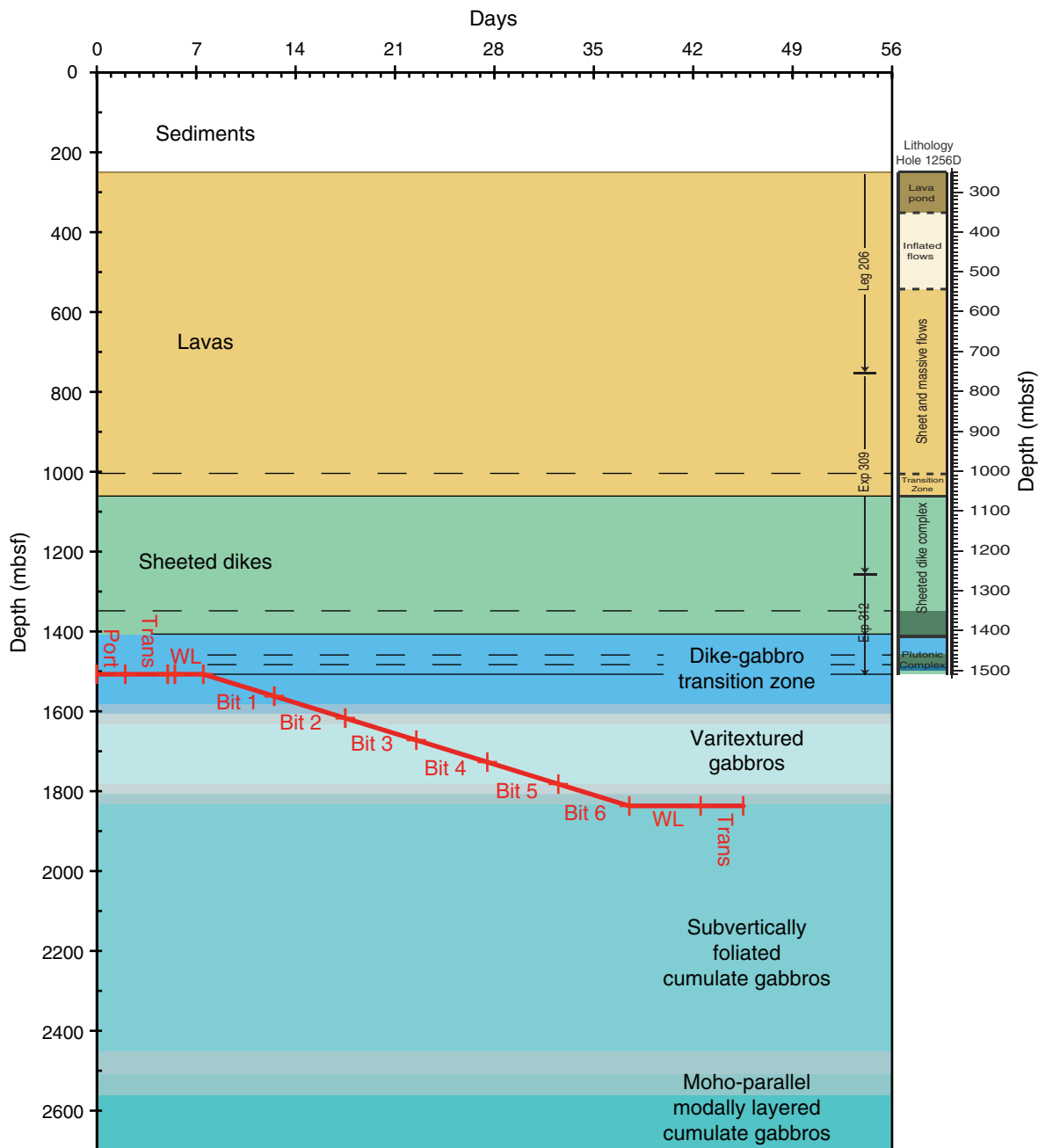
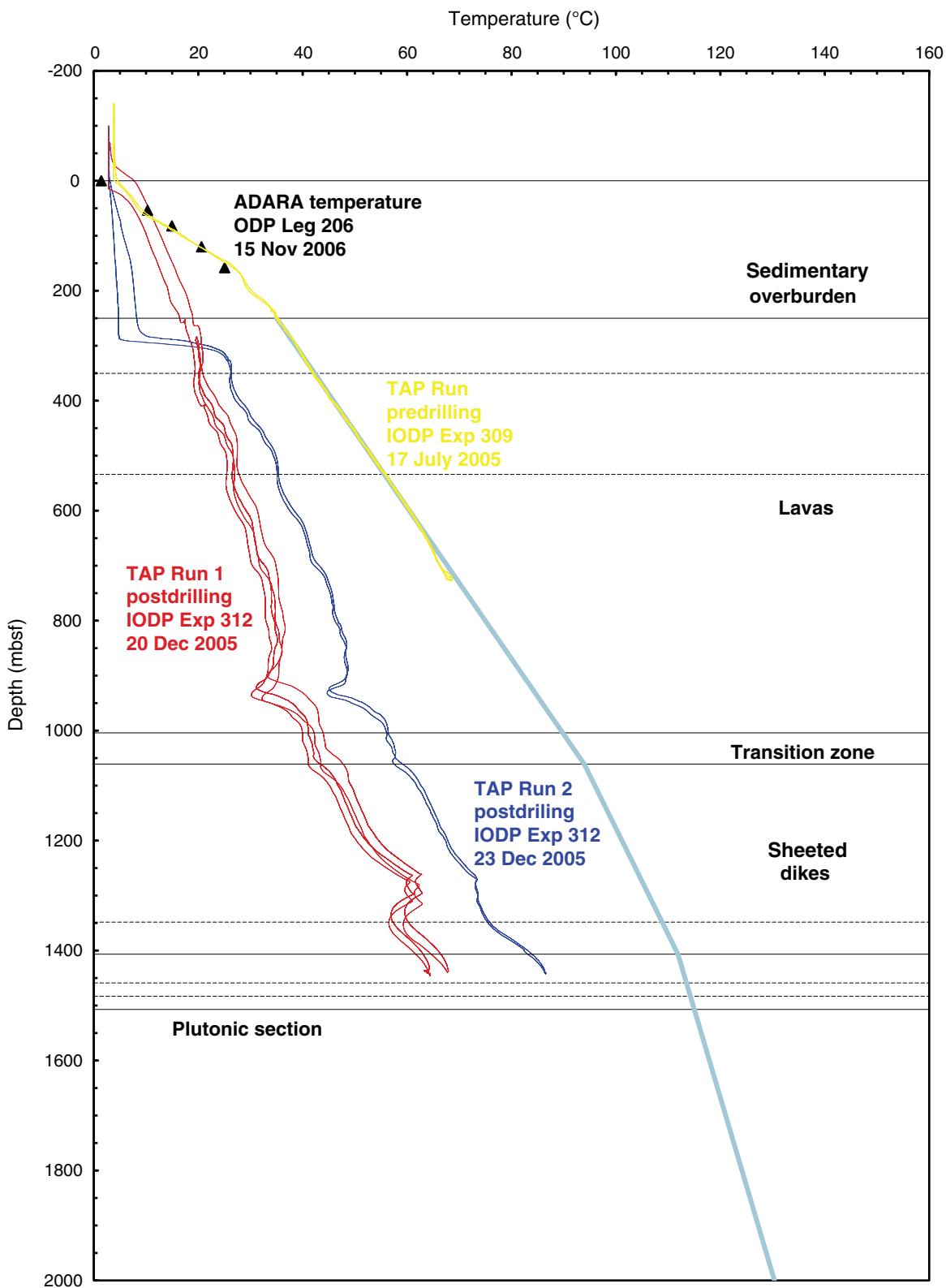


Figure F15. Measured and estimated temperatures with depth in Hole 1256D. Thermal profile estimated using the measured conductive heat flow and appropriate thermal conductivities for lavas, dikes, and gabbros.



Site summary

Site 1256 (GUATB-03C)

Priority:	1
Position:	6°44.19'N, 91°56.06'W
Water depth (m):	3635
Target drilling depth (mbsf):	As deep as possible
Approved maximum penetration (mbsf):	As deep as possible (EPSP reports as approved as proposed, and proposal requests >1700 m total penetration)
Survey coverage (track map; seismic profile):	<p>Acquired during <i>Ewing</i> cruise EW9903, March–April, 1999:</p> <ul style="list-style-type: none"> • MCS with 480 channels, 10 air guns • Refraction shooting 20 air guns recorded on ocean bottom hydrophones (OBHs) • 3.5 kHz reflection • Hydrosweep multibeam bathymetry • Site 1256 (proposed site GUATB-03C) is at the crossing of EW9903 Lines 22 and 27 (see Fig. F6).
Objective(s):	<ul style="list-style-type: none"> • Provide a reference with in situ samples through the extrusive volcanic and feeder dike section and into gabbroic rock in normal, intact oceanic crust formed at a very fast spreading rate at 15 Ma to constrain models of formation and alteration of oceanic crust. • Maintain a “legacy hole” available for future deepening.
Drilling program:	Continuous coring as deep as possible
Logging program: OR Downhole measurements program:	<ul style="list-style-type: none"> • Triple combo including MMT to determine borehole condition and temperature. If borehole has notably deteriorated, we may elect to conduct more logging runs with additional tools. If conditions permit, water sampling using WSTP. • Full logging suite planned at the end of the expedition includes the following: <ul style="list-style-type: none"> Triple combo FMS-sonic UBI: acoustic borehole images VSI: normal-incidence vertical seismic profiling MTT, HRLA, and HNGS: final temperature measurement Final triple combo for second temperature log
Nature of rock anticipated:	Gabbros and dikes

Expedition scientists and scientific participants

The current list of participants for Expedition 335 can be found at iodp.tamu.edu/scienceops/expeditions/superfast_rate_crust.html.